Large-scale integrated subglacial drainage around the former Keewatin Ice Divide, Canada reveals interaction between distributed and channelised systems

5   Emma L.M. Lewington[1], Stephen J. Livingstone[1], Chris D. Clark[1], Andrew J. Sole[1]
and Robert D. Storrar[2]

[1] Department of Geography, University of Sheffield, Sheffield, UK

[2] Department of Natural and Built Environment, Sheffield Hallam University, Sheffield, UK

Abstract

We identify and map traces of subglacial meltwater drainage around the former Keewatin Ice Divide, Canada from ArcticDEM data. Meltwater tracks, tunnel valleys and esker splays exhibit several key similarities, including width, spacing, their association with eskers and transitions to and from different types, which together suggest they form part of an integrated drainage signature. We collectively term these features 'meltwater corridors' and propose a new model for their formation, based on observations from contemporary ice masses, of pressure fluctuations surrounding a central conduit. We suggest that eskers record the imprint of a central conduit and meltwater corridors the interaction with the surrounding distributed drainage system. The widespread aerial coverage of meltwater corridors (5-36 % of the bed) provides constraints on the extent of basal uncoupling induced by basal water pressure fluctuations and variations in spatial distribution and evolution of the subglacial drainage system, which will modulate the ice dynamic response.

1. Introduction

Variations in the configuration of subglacial hydrological systems are key to understanding some of the most dynamic ice sheet behaviour at a range of spatial and temporal scales (e.g. Zwally et al., 2002; Das et al., 2008; Joughin et al., 2008; van de Wal et al., 2008; Shepherd et al., 2009; Palmer et al., 2011; Fitzpatrick et al., 2013; Doyle et al., 2014). Once water reaches the bed, its impact on ice flow is determined

by the hydraulic efficiency of the subglacial hydrological system. Theory developed at alpine glaciers suggests that increasing water pressure results in enhanced ice motion owing to reduced ice-bed contact (Lliboutry, 1968; Bindschadler, 1983) and where
40   sediment is present, enhanced sediment deformation (e.g. Engelhardt et al., 1978; Hodge, 1979; Iken and Bindshadler, 1986; Fowler, 1987; Iverson et al., 1999; Bingham et al., 2008). Water pressure at the bed depends on water supply to, storage within and discharge through the subglacial hydrological system (Iken et al., 1983; Kamb et al., 1985; Nienow et al., 1998). Hydraulically efficient drainage can accommodate and
45   evacuate greater meltwater flux with fewer and smaller spikes in basal water pressure, and thus has less impact on ice motion.

Traditionally the subglacial hydrological system has been conceptualised as a binary model comprising (i) inefficient distributed drainage - taking the form of thin
50   films of water (Weertman, 1972), linked cavities (Lliboutry, 1986; Walder, 1986; Kamb, 1987), groundwater flow (Boulton et al., 1995) and / or wide shallow canals (Walder and Fowler, 1994); and (ii) efficient channelised drainage with conduits cut either up into the ice (Rothlisberger-channel) or down into the bed (Nye-channel) (e.g. Rothlisberger, 1972; Shreve, 1972; Nye,1973; Hooke et al., 1990). While initially
55   proposed as independent elements, these two configurations are now thought to be frequently and extensively connected (e.g. Hubbard et al., 1995; Andrews et al., 2014).

In theory, in a steady-state system, water flows from surrounding high pressure distributed regions into lower pressure conduits. Borehole measurements of subglacial
60   water pressure, modelling and ice velocity proxy data (e.g. Hubbard et al., 1995; Gordon et al., 1998; Bartholomaus et al., 2008; Werder et al., 2013; Tedstone et al., 2014) suggest, however, that given a sufficiently large and rapid spike in water delivery to a subglacial conduit, the hydraulic gradient can be reversed such that water is forced out and laterally away from the conduit across a zone some metres to several
65   kilometres wide that has been referred to as a Variable Pressure Axis (VPA) (Hubbard, 1995). Thus, during significant fluctuations in the delivery of surface water to the bed, conduits interact with their surroundings, supporting the notion of a three-system model of: channelised subglacial drainage connected to the supraglacial hydrological system; distributed subglacial drainage weakly connected to the subglacial channels;
70   and hydraulically isolated subglacial distributed drainage (Hoffman et al., 2016).

Despite these advances in understanding, observations of distributed and channelised drainage interactions are sparse, and so controls on their spatial distribution and temporal evolution remain poorly constrained.

1.1 Palaeo-meltwater landforms

Palaeo–meltwater landforms have been fundamental in inspiring and guiding conceptual and numerical models of how water self-organises into drainage systems beneath present day ice masses because they can be easily observed and investigated. Such landforms are therefore key to contextualising spatially and temporally limited contemporary observations and are commonly used to support and develop the theory of ice sheet hydrological systems (e.g. Shreve, 1985; Clark and Walder, 1994; Boulton et al., 2007a,b; 2009; Hewitt and Creyts, 2019). Much of this focus has been on landforms such as eskers, meltwater channels and tunnel valleys which indicate efficient channelised subglacial drainage (e.g. Shreve, 1985; Brennand, 1994, 2000; Clark and Walder, 1994; Punkari, 1997; Boulton et al., 2007a, b, 2009; Storrar et al., 2014a; Livingstone and Clark, 2016). We will now discuss each of these in more detail.

1.1.1 Eskers

Eskers are linear depositional landforms made up of glaciofluvial sand and gravel deposited from meltwater flowing through an ice mass in conduits metres to tens of metres in width and height. They exist as individual segments that often align to form networks extending up to several hundreds of kilometres (e.g. Shreve, 1985; Aylsworth and Shilts, 1989; Brennand, 2000; Storrar et al., 2014a; Stroeven et al., 2016) and are typically taken to record the former position and characteristics of Röthlisberger-channels (R-channels) thermally eroded into the base of the ice by turbulent water flow. While most studies reduce esker mapping to a single crest-line and consider the 'classic' single straight-to-sinuous undulating ridge to be pervasive, more complex esker morphologies also occur (e.g. Banerjee and McDonald, 1975; Rust and Romanelli, 1975; Hebrand and Amark, 1989; Gorrell and Shaw, 1991; Warren and Ashley, 1994; Brennand, 2000; Mäkinen, 2003; Perkins et al., 2016; Storrar et al., 2019). These include fine-grained sandy fan shape elements or 'splays',

105   alongside and associated with the coarse gravelly central ridge (e.g. Cummings et al.,
       2011a; Prowse, 2017). These splays are an order of magnitude wider and more gently
       sloped than the main ridge (Cummings et al., 2011a). They are proposed to form in
       both proglacial environments, representing subaqueous outwash fans deposited by
       sediment laden plumes exiting a subglacial conduit into a proglacial lake (e.g. Powell,
110   1990; Hoyal et al., 2003; Cummings et al., 2011b), and / or subglacial environments,
       with sedimentation in subglacial cavities alongside the main esker ridge during periods
       of conduit over-pressurisation (e.g. Gorrell and Shaw, 1991; Brennand, 1994).

1.1.2 Meltwater channels and tunnel valleys

115

       Erosional subglacial meltwater channels, or Nye-channels, incised into bedrock or
       sediment substrate range in size from metres to tens of metres wide (e.g. Sissons,
       1961; Glasser and Sambrook Smith, 1999; Piotrowski, 1999) to large tunnel valleys
       several kilometres in width and tens of kilometres long (e.g. Kehew et al., 2012; van
120   der Vegt et al., 2012; Livingstone and Clark, 2016). Tunnel valleys are observed to
       occur at various developmental stages from mature and clearly defined to indistinct
       valleys often associated with hummocky terrain or as a series of aligned depressions
       (e.g. Kehew et al., 1999; Sjogren et al., 2002). Their formation has been linked to
       subglacial meltwater erosion at the ice-bed interface (c.f. Ó Cofaigh, 1996; Kehew et
125   al., 2012; van der Vegt et al., 2012) with the assumption that channels transported
       large volumes of sediment and water. However, their precise mechanism of formation
       is still debated with the main arguments focussing on i) catastrophic outburst formation
       with rapid erosion following the release of sub or supraglacially stored water (e.g.
       Piotrowski, 1994; Cutler et al., 2002; Hooke and Jennings, 2006; Jørgensen and
130   Sandersen, 2006) and ii) gradual steady-state formation with headward erosion of
       soft-sediments in low water pressure conduits (e.g. Boulton and Hindmarsh, 1987;
       Mooers, 1989; Praeg, 2003; Boulton et al., 2009).

       Here, we use the term meltwater channel to refer to palaeo-evidence of erosional
135   channelised flow left on the ice sheet bed (i.e. the outline of the path the water took)
       at all scales from N-channels through to tunnel valleys. We use the term conduit to
       refer to the active channelised flow beneath a contemporary ice mass (i.e. the
       enclosed (sediment and / or ice walled) pipe carrying water at the ice-bed interface).

1.1.3 Meltwater tracks

140

Detailed mapping in northern Canada and Scandinavia has identified the presence of linear tracks variously termed 'hummock corridors', 'glaciofluvial corridors', 'washed zones' and 'esker corridors', typically a few hundred meters to several kilometres wide and a few kilometres to hundreds of kilometres long (e.g. St-Onge, 1984; Dredge et

145   al., 1985; Rampton, 2000; Utting et al., 2009; Burke et al., 2012; Kerr et al., 2014a, 2014b; Sharpe et al., 2017; Peterson et al., 2017; Peterson and Johnson, 2018; Lewington et al., 2019). These features often contain eskers and hummocks which vary in size, shape and relief (Peterson and Johnson, 2018) as well as 'patches' of glaciofluvial deposits and areas of exposed bedrock. While a subglacial meltwater

150   origin is largely agreed upon, their precise mode of formation is not yet known. These features are collectively termed meltwater tracks hereon in.

Meltwater landforms are typically mapped and interpreted individually (e.g. Clark and Walder, 1994; Brennand, 2000; Storrar et al. 2013; Burke et al., 2015; Livingstone

155   and Clark, 2016; Mäkinen et al., 2017) rather than as a holistic drainage signature (c.f. Storrar and Livingstone, 2017). As such, it is not yet clear whether or how differing expressions of subglacial drainage are interrelated and to what extent variations in drainage and / or background conditions (e.g. bed substrate, geology and local topography) control the preserved geomorphic signature we see today. This study

160   aims to identify and map all discernible evidence of subglacial meltwater drainage across the Keewatin District of northern Canada from the ArcticDEM. We collectively refer to these as meltwater routes (MW_{Routes}). Producing an integrated map of all visible subglacial meltwater evidence allows us to report on the varying dimensions and geomorphological expressions of these features, to investigate associations

165   between features traditionally treated separately and to explore potential controls on expression and formation.

2. Study Area

170   This study focusses on an area approximately 1 million km^2 to the west of Hudson Bay in northern Canada that surrounds the location of the former Keewatin Ice Divide (Fig. 1) (Lee et al., 1957; McMartin et al., 2004). The area generally exhibits low relief

and is underlain by resistant Precambrian bedrock that is either exposed or covered
by till ranging from thin and discontinuous to thick and pervasive (e.g. Clark and
175   Walder, 1994).
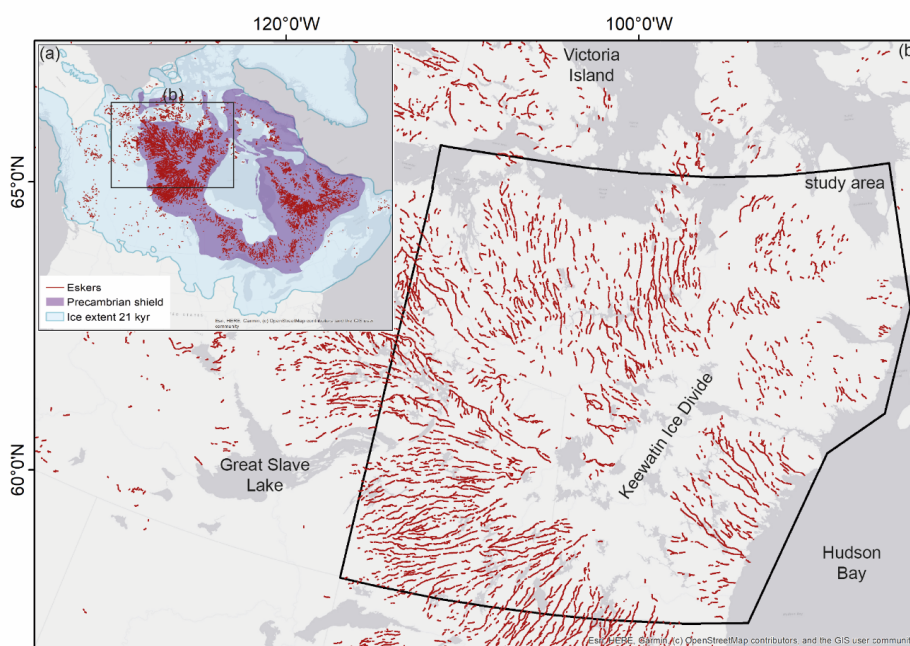
Figure 1. (a) Large-scale distribution of eskers around Hudson Bay (Storrar et al., 2013). The
Laurentide Ice Sheet extent displayed in the inset is the Last Glacial Maximum (LGM) at 18
[14]C ka BP (21.4 cal. ka BP) (Dyke et al., 2003) and the extent of the Precambrian shield is
180   also mapped (Wheeler et al., 1996). (b) Zoomed in location of the study area focussed on the
area around the former Keewatin Ice Divide.

         Traditionally, eskers have been identified as the predominant meltwater
landform within the Keewatin area, although meltwater tracks (MW_{Tracks}) (e.g. St-
185   Onge, 1984; Aylsworth and Shilts, 1989; Rampton, 2000; Utting et al., 2009; Sharpe
et al., 2017; Lewington et al., 2019) and meltwater channels (e.g. Storrar and
Livingstone, 2017) have also been recorded. At a large scale, eskers radiate out from
the ice divide, beneath which they are rare (Shilts et al., 1987; Aylsworth and Shilts,
1989; Storrar et al., 2013, 2014a). At a local to regional scale, they exhibit a dendritic
190   pattern and 12–15 km quasi-uniform spacing (e.g. Banerjee and McDonald, 1975; St-
Onge, 1984; Shilts et al., 1987; Bolduc, 1992; Storrar et al., 2014a).

Eskers have been widely mapped in northern Canada. Initial mapping was largely undertaken by the Geological Survey of Canada using air photography and field observations (e.g. Aylsworth and Shilts, 1989). This included mapping of 'esker systems' - comprising a series of hummocks or short, flat-topped segments which phase downstream into relatively continuous esker ridges or occasionally beaded eskers - across 1.3 million km^2 of the Keewatin sector of the Laurentide Ice Sheet (LIS) (Aylsworth and Shilts, 1989; Aylsworth et al., 2012). Discontinuous esker ridges are connected to areas of outwash, meltwater channels or belts of bedrock stripped free of drift. More recently, increasing availability of remotely sensed data allowed Storrar et al., (2013) to digitise eskers at an ice sheet scale for the LIS (including the Keewatin sector) using Landsat 7 ETM+ imagery. From this, a secondary dataset was derived by interpolating a straight line between successive aligned esker ridges, creating a continuous pathway, which reflects the location of the major conduits in which the eskers formed (Storrar et al., 2014a).

3. Methods

3.1 Data sources and mapping

ArcticDEM 10 m resolution DEMs (freely available at https://www.pgc.umn.edu/data/arctcidem), generated by applying stereo and auto-correlation techniques to overlapping pairs of high-resolution optical satellite images (Noh and Howat, 2015; Porter et al., 2018), were used in this study to identify and map meltwater landforms. Eskers mapped by Storrar et al. (2013) from 30 m resolution Landsat ETM+ multispectral imagery were used to inform further high-resolution esker mapping from the 10 m resolution DEM. The automatic mapping approach developed in Lewington et al. (2019) was used to create a first pass map of hummock corridors – classified as meltwater tracks here (Appendices Fig. A1) to augment the improved esker map. Together, these were used to create an integrated map of MW$_{Routes}$ by manually mapping centrelines of all visible traces of subglacial meltwater drainage including meltwater tracks, meltwater channels and eskers. Multiple orthogonal hillshades were generated to avoid azimuth bias (Smith and Clark, 2005) and mapping was undertaken at a range of spatial scales to maximise the number of features captured (Chandler et al., 2018).

3.2. Classification and morphometry

The MW$_{Routes}$ were used to explore the occurrence and morphology of different
types of meltwater landforms. Former ice-margin estimates from Dyke et al. (2003)
were used as transects. These transects are spaced approximately 30–40 km apart
and in the study area, cover c. 1,000 years of deglaciation between 9.7 and 8.6 ka.
This period encompasses the final stages of deglaciation when the ice sheet was
experiencing a strongly negative surface mass balance with associated increasing
rates of meltwater production (e.g. Carlson et al., 2008, 2009). Retreat rates were
generally between 100-200 m yr^{-1} from 13 to 9.5 ka, increasing rapidly between 9.5
and 9 ka to around 400 m yr^{-1} after which retreat rate decreased briefly before another
increase from ~8.5 ka (Dyke et al., 2003).

When a MW$_{Route}$ intersected a transect, an intersection point was added, and
the following information recorded:

- Landform type (i.e. esker ridge, esker with lateral splay, meltwater track or
  meltwater channel)
- Width of landform (or landforms if an esker ridge was present within a meltwater
  track, meltwater channel or surrounded by a lateral splay)
- Bed substrate and geology (Fulton, 1995; Wheeler et al., 1996).

Spacing between adjacent MW$_{Route}$ centrelines was calculated along each transect
with centrelines at the end of each transect and those separated by clear breaks (e.g.
due to the coincidence of a lake) discounted. The total length of MW$_{Route}$ centrelines
was calculated automatically in a GIS.

3.3 Testing controls on MW$_{Routes}$ width and expression

This study takes a large-scale approach to exploring controls on MW$_{Routes}$ width
and expression. While this approach results in a compromise in terms of data
resolution available for the surface substrate and geology maps, it also increases
statistical confidence in the results due to the larger sample size. Before analysis was

260   undertaken, three test sites were selected from the study area to allow for more detailed mapping and comparisons (Appendices Figs. A2 and A3).

        To explore substrate and geological controls on MW_{Route} occurrence, distribution and properties, the overall length of MW_{Routes} overlying each substrate type

265   (Fulton, 1995) and geology (Wheeler et al., 1996) within the three test sites was calculated. The total area of each basal unit within the test sites was also calculated and values converted to percentages. Following this, the percentage area was subtracted from the percentage of MW_{Routes} for each individual substrate and geology type, giving a positive (over-represented) or negative (under-represented) value. Next,

270   MW_{Routes} were split and classified by feature expression (i.e. esker, esker with lateral splay, glaciofluvial material, anabranching sections, meltwater channel and MW_{Track}). The above analysis was repeated by feature type to explore whether geomorphological expression is controlled by surface substrate / geology. It is important to note that categorisations along MW_{Routes} were not always independent as

275   the same section was sometimes coded as a meltwater track and an esker with splay / glaciofluvial deposits as often 'positive' features are situated within wider erosional corridors.

        It was noted that landform type varies both across adjacent MW_{Routes} and along

280   individual MW_{Route} centrelines. To assess any potential relationship between landform expression and background controls in more detail, individual centrelines were selected and sampled with a higher frequency (5 km intervals). At each sample point the width of the MW_{Track} / meltwater channel, the presence / absence of an esker (and its width if present), surface substrate, bed geology and elevation were recorded.

285

        To investigate the relationship between subglacial drainage and bed roughness, the standard deviation of the ArcticDEM (resampled to 50 m) was calculated using a 1 km and 5 km radius circular search window and this was compared to the density of MW_{Routes}. Ice stream locations (Margold et al., 2015) were

290   also qualitatively compared to the distribution of MW_{Routes}.

4. Results

295 **4.1 An integrated drainage signature**

Mapping all traces of meltwater drainage reveals the ubiquity of former subglacial drainage across the study area (Fig 2). A total of 2,795 MW_{Routes} were mapped over a ~1 million km^2 area with a total length of 51,856 km. The MW_{Routes} exhibit a similar overall pattern to earlier esker maps (e.g. Aylsworth and Shilts, 1989; Storrar et al.,

300   2013) radiating out from the former Keewatin Ice Divide. Greater than 90 % of mapped esker ridges in this region are estimated to occur along a MW_{Route} and therefore form part of this wider network of drainage features. In terms of the large-scale pattern, there are no obvious trends in MW_{Route} density, width or feature type

305   associated with margin retreat. However, the study area only covers approximately 1,000 years, associated with a period of intense meltwater production and rapid retreat.
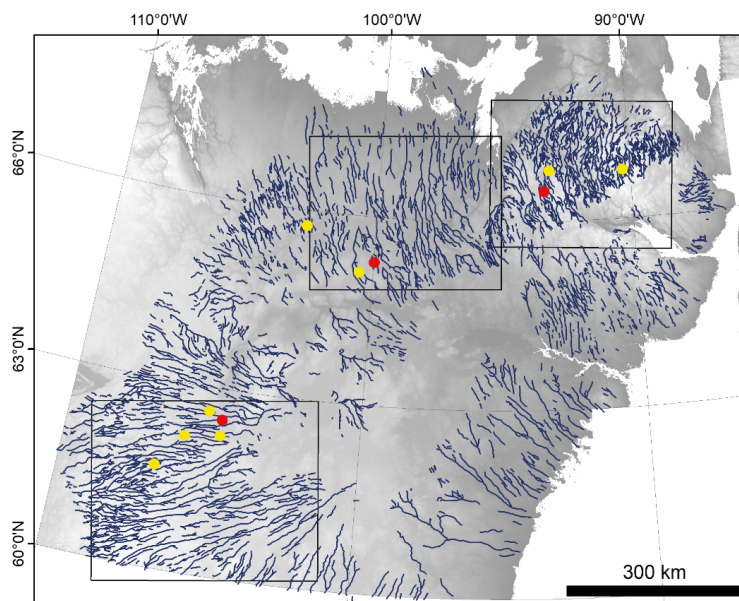
Figure 2. Integrated map of MW_{Routes}. Note how MW_{Routes} in this new map are less fragmented

310   and denser than the existing esker map (Fig. 1b). Red points represent examples in Fig. 4 and yellow points those in Fig. 5. DEM created by Canadian Digital Elevation Model (CDEM). Ottawa, ON: Natural Resources Canada [2015].

Esker ridges are recorded at 43 % of all sample points. Where they do occur, 87 % of them are flanked by a wider meltwater track, channel or splay. Comparing the updated esker map to the new MW_{Routes} map presented here confirms the large-scale association between eskers and wider meltwater features which often flank and / or connect intervening segments (Fig. 3). A wider meltwater feature in the scale of 100s-1000s m was recorded at 90 % of sample points (the remaining 6 % captured an esker ridge alone and 4 % were considered ambiguous and therefore not classified). This suggests that the mapping of complete MW_{Routes} creates a more complete and less fragmented drainage map with a higher number of tributaries and greater overall density, particularly in the Nunavut area (Fig. 3c). Nonetheless, evidence of palaeo-drainage remains noticeably absent beneath the location of the former ice divide (Fig. 2).

Table 1. Summary statistics for MW_{Routes} in the study area.

	Length (km)	Width (km)	Spacing (km)
Min	0.7	0.05	0.4
LQuartile	4.9	0.5	3.3
UQuartile	20.7	1.1	10.1
Max	339.9	3.3	77.9
Mean	18.5	0.9	8.1
Std dev.	26.9	0.6	7.4

MW_{Routes} reach a maximum of 340 km in length and 3.3 km in width (Table 1), but are noted to reach up to 760 km when they extend beyond the limits of the study area (Storrar et al., 2014a). Meltwater channels and meltwater tracks are typically an order of magnitude wider (mean width: 900 m) than the eskers which they often contain (mean width: 97 m). MW_{Routes} appear to vary in width around the ice sheet and along individual centrelines but show no clear (temporal) trend from the ice divide towards the margin. Within the study area, adjacent centrelines are spaced on average 8 km apart (Table 1). This is at the lower end of the range that has been observed and modelled (e.g. Banerjee and McDonald, 1975; St-Onge, 1984; Shilts et al., 1987; Hebrand and Amark, 1989; Bolduc, 1992; Boulton et al., 2009; Hewitt, 2011). Like variations in width, there appears to be no coherent change in spacing over time within this area (Fig. 3).

4.2 Comparison to previous regional – large scale mapping
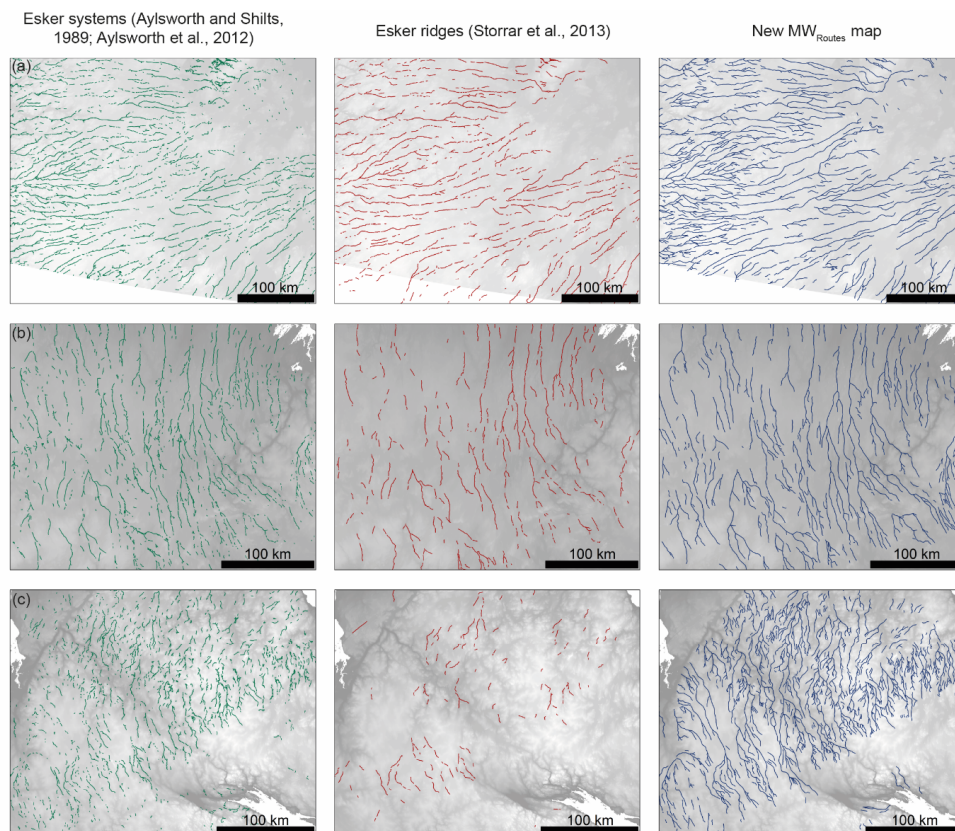
345 **Figure 3.** Comparison of existing mapping of 'esker systems' (green) from air photo interpretation (Aylsworth and Shilts, 1989; Aylsworth et al., 2012), esker ridges (red) from Landsat imagery (Storrar et al., 2013) and the new MW$_{Routes}$ from the ArcticDEM (blue). Mapping of MW$_{Routes}$ includes all traces of subglacial meltwater flow i.e. eskers, eskers with lateral splay, meltwater tracks and meltwater channels. The locations of (a) (test site 1), (b) 350 (test site 2) and (c) (test site 3) are identified in Fig. 2. DEM(s) created from the Canadian Digital Elevation Model (CDEM). Ottawa, ON: Natural Resources Canada. [2015]

This paper extends earlier work which recognises links between eskers and 355 broader traces of subglacial meltwater flow but does not explicitly describe or formally

quantify them (e.g. Aylsworth and Shilts, 1989; Storrar et al., 2014a). It is encouraging that despite different datasets and mapping procedures, the overall patterns are similar (Fig. 3). Here we go beyond mapping eskers alone and identify and classify each part of the MW$_{Routes}$, including those which do not contain an esker. We describe

360   them in detail (section 4.3) and explore the role of background controls in influencing geomorphic expression (section 4.4), providing insight into the drainage system operation (section 5).

4.3 Geomorphological variations

365

Landforms along MW$_{Routes}$ exhibit a high degree of geomorphic variability in terms of relief and definition (Fig. 4). Some exhibit strongly negative relief (down to ~30 m below their immediate surroundings) and distinct boundaries, i.e. meltwater channels (Fig. 4a and 4c), while others exhibit negligible relief and are more difficult to

370   differentiate from their surroundings i.e. meltwater tracks (e.g. Fig. 4d and 4e) or even exhibit positive relief i.e. eskers with lateral splay (e.g. Fig. 4f, 4g and 4h). Channel edges vary from straight to crenulated and from continuous to discontinuous. A variety of forms are found within the meltwater tracks and meltwater channels. These include hummocks of varying size, shape and relief and eskers and associated glaciofluvial

375   material (e.g. Fig. 4e and 4f). In places, till may be entirely eroded revealing patches of bedrock. Eskers display a higher degree of variability along the MW$_{Routes}$ with single, continuous straight-to-sinuous ridges the exception rather than the norm (e.g. Fig. 4a and 4b).
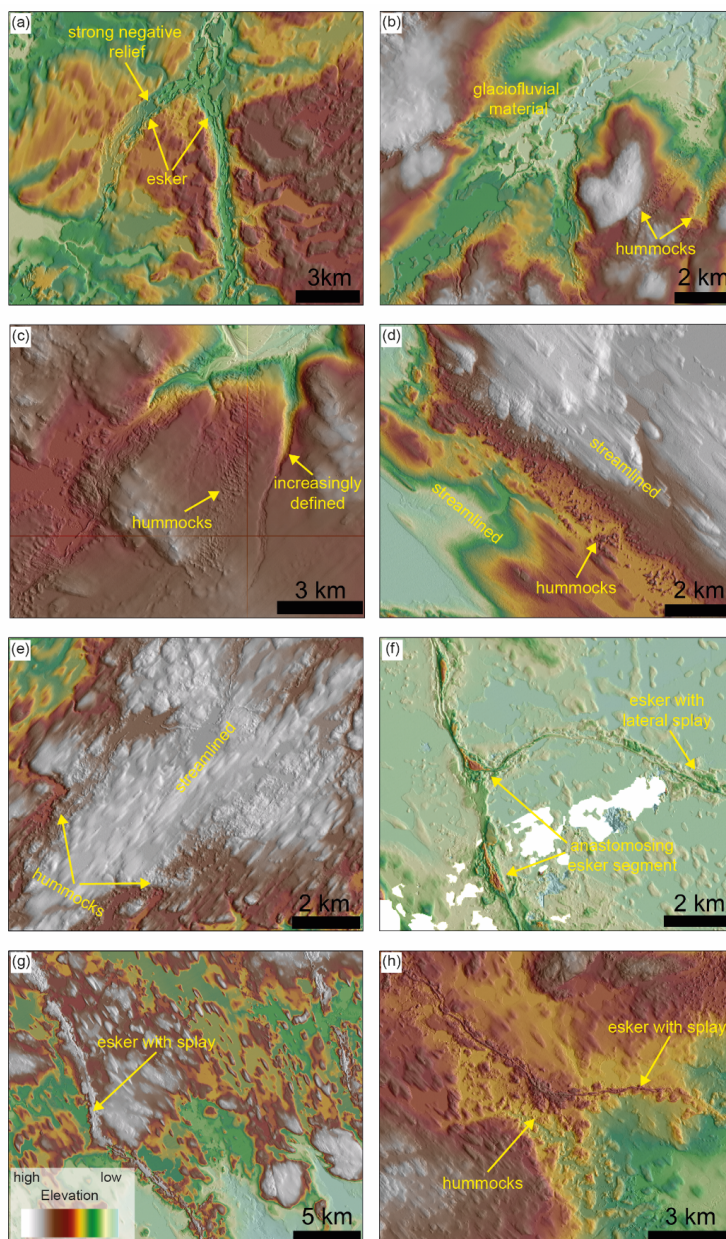
380

Figure 4. Different geomorphological expressions observed along MW$_{routes}$ in the Keewatin sector of the Laurentide Ice Sheet: (a-c) negative relief features with hummocks, eskers and glaciofluvial material within. They also demonstrate how features can vary in expression over short distances. (d-e) moderate to negligible relief features, defined by the presence of

385 hummocks which stand out from the surrounding streamlined terrain. (f) two MW$_{Routes}$ with

multiple sections of anastomosing eskers which join into a single feature downstream. (g) lateral splay surrounding a central esker ridge. (h) esker with splay joining a MW$_{Track}$ from the SE perhaps indicating multiple stages of flow. DEM(s) created by the Polar Geospatial Center from DigitalGlobe, Inc. imagery.

390

Geomorphological expression varies both across flow (i.e. between adjacent centrelines) and along flow (i.e. along individual centrelines). Variations in landforms are recorded along individual MW$_{Routes}$ by multiple transitions to and from landform
395   classifications. Figure 5 shows examples of downstream transitions from meltwater channels to eskers with lateral splay (e.g. Fig 5a) and from meltwater channels to meltwater tracks and back (e.g. Fig. 5b and 5c).
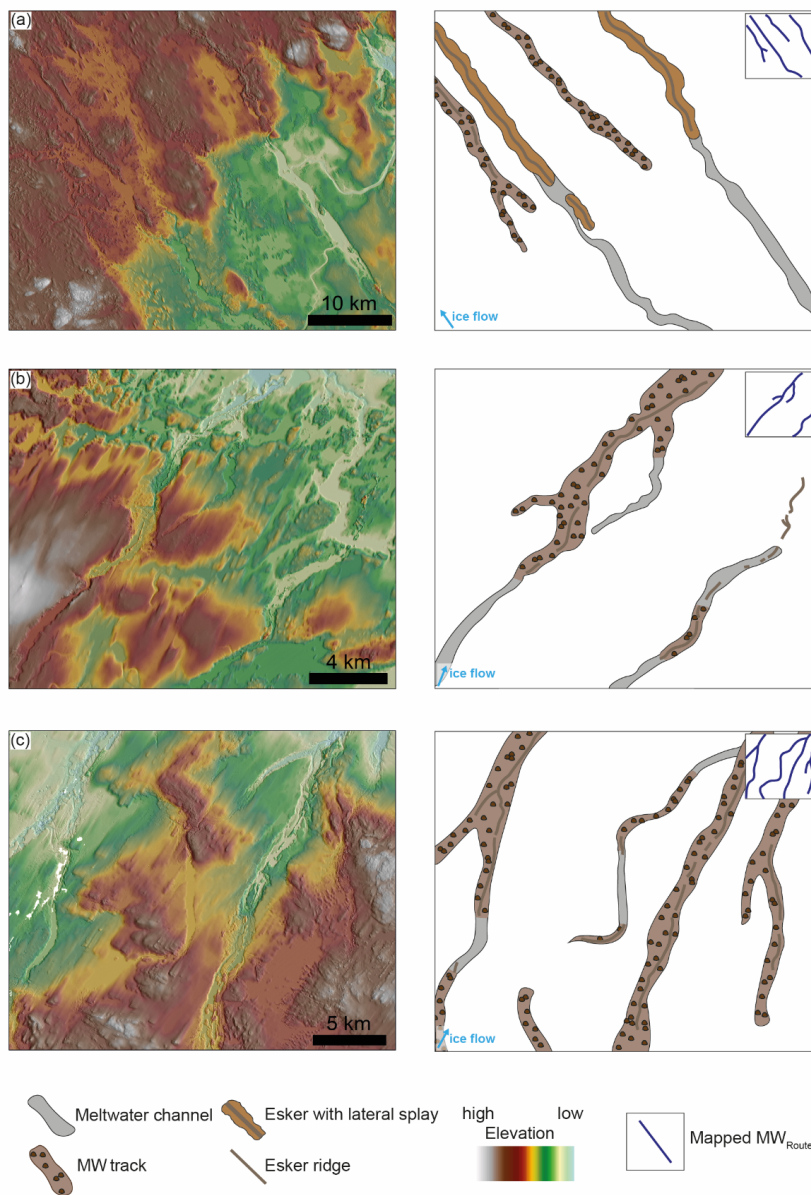
Figure 5. Examples of transitions and associations along MW$_{Routes}$. The left panel shows the DEM and the right panel shows an interpretation of the feature types with an inset (top right) showing how MW$_{Routes}$ are mapped as single lines through all types. White patches in the DEM represent areas of missing data due to the presence of hydrological features (e.g. lakes and rivers) and / or in areas of cloud cover and shadow. DEM(s) created by the Polar Geospatial Center from DigitalGlobe, Inc. imagery.

Despite variations in expression (e.g. relief, definition and the presence or absence of hummocks, glaciofluvial material and/ or eskers), meltwater tracks, meltwater channels and eskers with lateral splays are all associated with eskers (Fig. 4) and form an integrated and coherent large-scale spatial pattern (Fig. 5).

410 Furthermore, they display a qualitatively similar width range - several hundred meters to ~3 kilometres (Fig. 6) – although, the null hypothesis that the data in each pairing are from the same continuous distribution using the two-sample Kolmogorov-Smirnov test could not be rejected for any pairings (esker, esker with splay, meltwater channel and meltwater track) at the 5 % significance level.

415
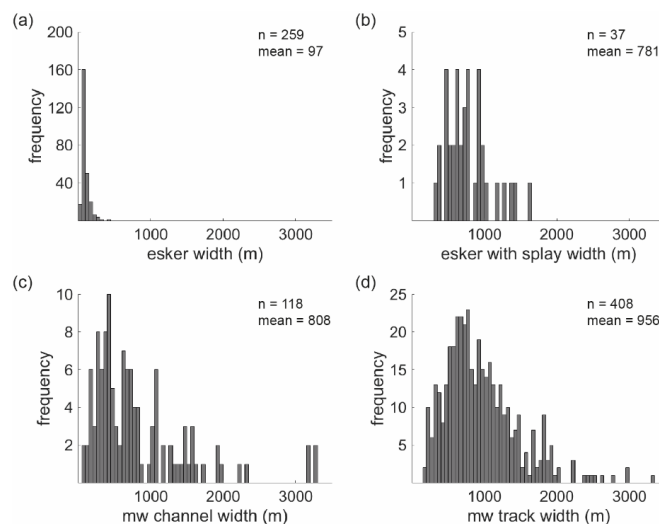
Figure 6. Width distributions (in metres) of (a) esker ridges, (b) eskers with lateral splay, (c) meltwater channels and (d) meltwater tracks. Note the similarity in distributions between
420 eskers with lateral splay, meltwater channels and meltwater tracks.

4.4 Controls on the width and expression of meltwater landforms

425 Most subglacial meltwater landforms occur within areas of till (Fig. 7). Meltwater tracks, eskers with lateral splays and meltwater channels are all overrepresented in areas of till blanket, while esker ridges are strongly underrepresented. Meltwater

features appear most commonly over areas of metamorphic bedrock, although
meltwater channels (incisional features) are overrepresented on more erodible
430   sedimentary rocks.
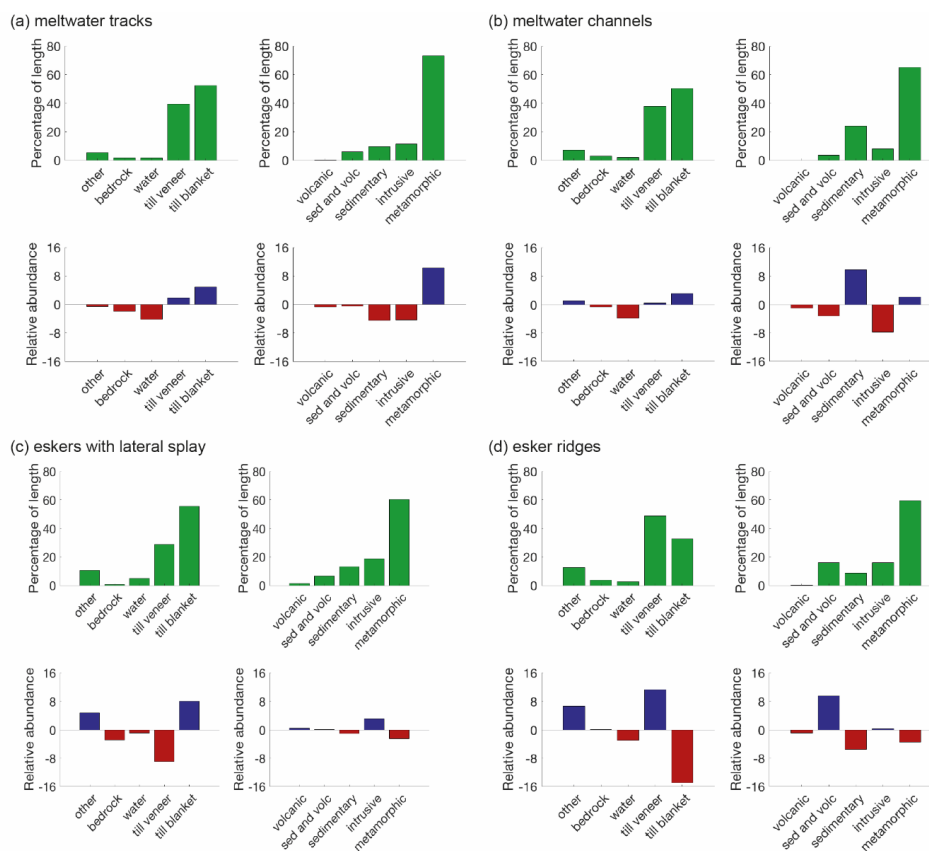
Figure 7. Substrate control on geomorphological expression. Occurrence (percentage of
length) and relative abundance of different meltwater features over varying surface substrates
435   (Fulton, 1995) and background geology (Wheeler et al., 1996). 'Other' includes marine,
lacustrine and glaciofluvial sediments.

Figure 8 reveals two areas with a high density of MW$_{Routes}$ – the largest in the NE
440   and the other in the SW. These coincide qualitatively with areas of high local
topographic variation (i.e. high standard deviation) at both scales of roughness

calculation (1 km and 5 km). Palaeo-ice streams are rare in the Keewatin District region (Stokes and Clark, 2003a,b; Margold et al., 2018), but where they do occur (e.g. Dubawnt Lake and Maguse ice streams), MW$_{Routes}$ are noticeably sparser and

445   more fragmented (Fig. 9). On the bed of the Dubawnt Lake Ice Stream, the MW$_{Routes}$ also exhibit a more dendritic arrangement and extend further towards the ice divide.
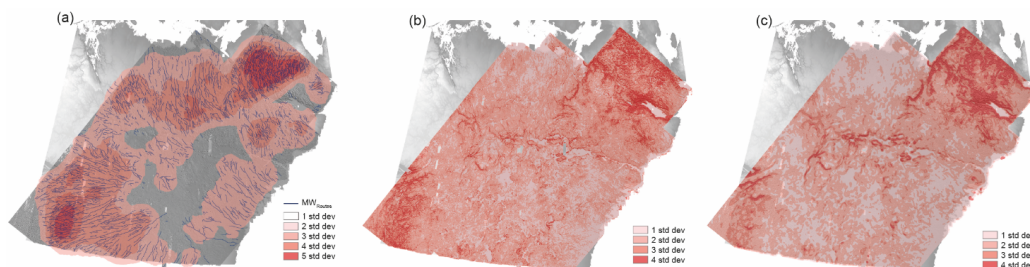
450   **Figure 8.** Density of MW$_{Routes}$ (a) compared to local bed roughness (standard deviation) using (b) 1 km and (c) 5 km search window where darker colours represent greater deviation from the mean. DEM(s) created by the Polar Geospatial Center from DigitalGlobe, Inc. imagery and the Canadian Digital Elevation Model (CDEM). Ottawa, ON: Natural Resources Canada. [2015].

455

To explore potential controls governing how meltwater landform expression varies with changing background conditions, detailed measurements of width, feature type and substrate were extracted along individual MW$_{Routes}$ (Fig. 10). Although there is no

460   consistent ratio between esker width and the associated meltwater track / meltwater channel width at sample points across the whole study area, qualitatively there is a positive relationship between the two, with both increasing and decreasing in phase (Fig. 10). Esker width varies along individual pathways (varying by almost 300 % (Fig. 10b)) and expressions range from a single well-defined ridge to multiple, fragmented

465   and anabranching sections. The MW$_{Route}$ in Fig. 10b suggests that wider sections broadly coincide with higher bed elevations and the presence of more deeply eroded, yet narrower sections with decreasing elevation. In Fig. 10d we observe a large increase in width associated with a rapid increase in elevation, which also coincides with a transition from a strongly negative feature (a meltwater channel) to a positive /

470   depositional feature (esker with lateral splay). This sharp transition is related to the
emergence of the MW$_{Route}$ out of the Thelon sedimentary basin.
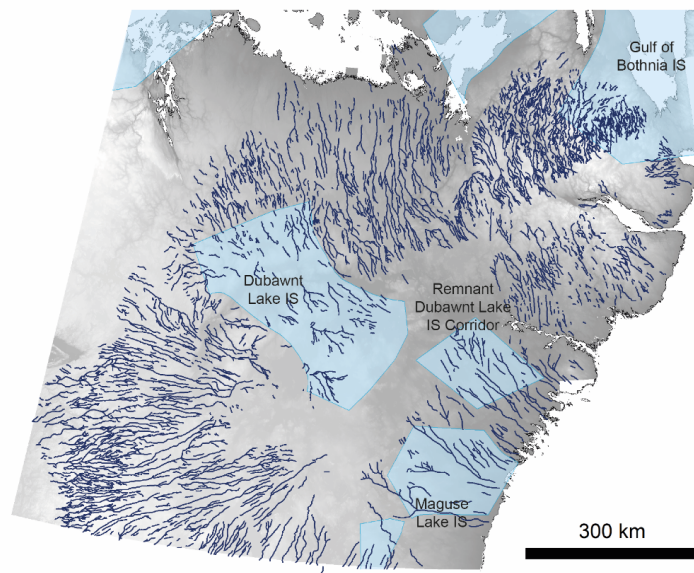
Figure 9. Comparison of MW$_{Routes}$ and palaeo-ice streams (Margold et al., 2015). Note that
the few palaeo-ice streams that do occur within our study area tend to be associated with
475   fewer MW$_{Routes}$. MW$_{Routes}$ on the bed of the Dubawnt Lake Palaeo-Ice Stream are also
distinctively more dendritic. DEM(s) created the Canadian Digital Elevation Model (CDEM).
Ottawa, ON: Natural Resources Canada. [2015].

480

485
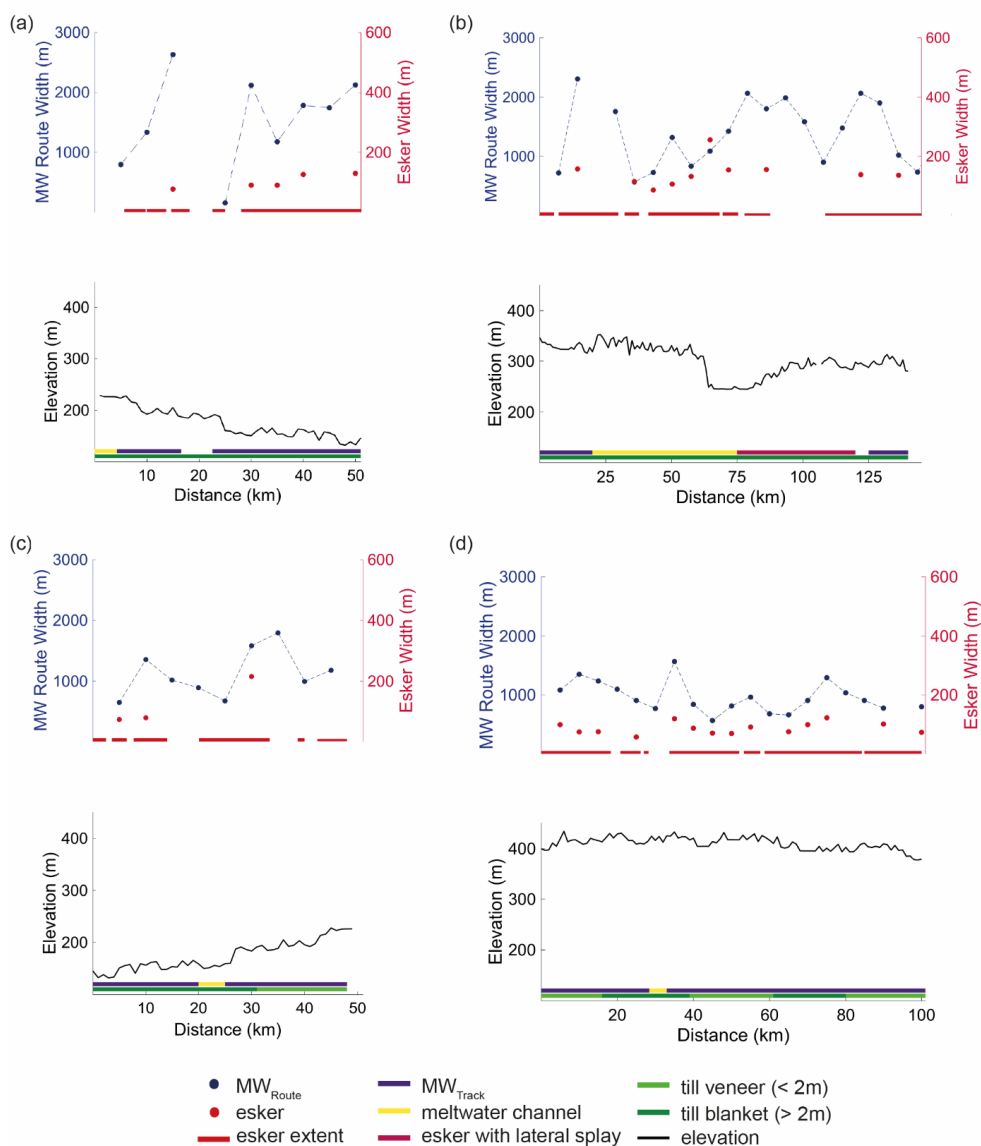
490

Figure 10. Exploring local-scale controls on MW$_{Route}$ width and expressions. Detailed profiles (sampled at 5 km intervals along individual MW$_{Routes}$) show how esker extent, elevation, feature expression and surface substrate vary along flow from the interior (left) to the exterior (right).

495

5. Discussion

Our new MW$_{Routes}$ map shows that meltwater tracks, meltwater channels and esker
splays which flank and connect (in an along-flow direction) esker ridges are a dominant
part of the landscape across the former Keewatin sector of the LIS. Mapping complete
drainage pathways means we are better able to identify regional meltwater drainage
patterns and unravel controls on feature expression.
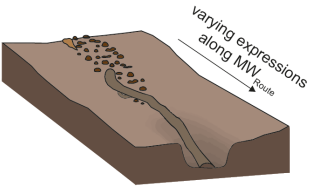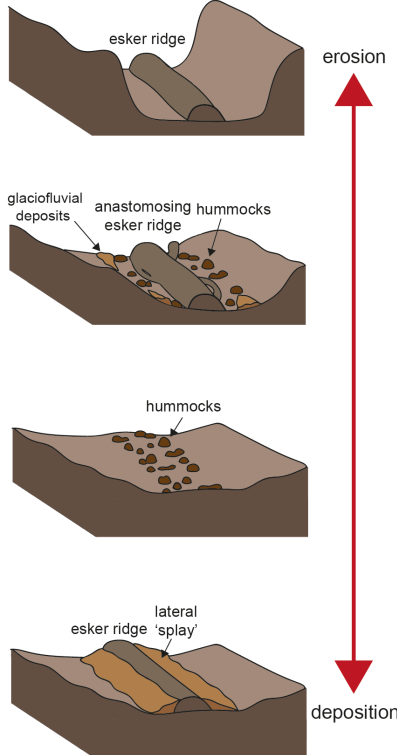
The large-scale distribution and pattern of meltwater tracks, channels and
eskers with lateral splays exhibit several key similarities, including their width, spacing,
association with eskers and occurrence within an integrated network characterised by
transitions to and from different types along individual MW$_{Routes}$ (Figs. 4-6). Together,
this provides strong evidence that these meltwater landforms are varying expressions
of the same phenomenon and we therefore collectively group these features with
widths in the order of 100s to 1000s of meters and term them meltwater corridors
(MW$_{Corridors}$) (Table 2). This is consistent with previous conceptual work linking
meltwater landforms. For example, Sjogren et al., (2002) identify various expressions
of tunnel valley (meltwater channel) that they attribute to different developmental
stages, from discontinuous through to fully developed valleys. Peterson and Johnson
(2018) suggest that negative relief hummock corridors (meltwater tracks) are a type of
tunnel valley and positive relief hummock corridors are the same as features
previously identified and termed 'glaciofluvial corridors' in Canada (e.g. Utting et al.,
2009).

530   **Table 2.** Proposed classification for subglacial meltwater traces observed on palaeo-beds. MW$_{Routes}$ encompasses all evidence and consists of MW$_{Corridors}$ i.e. all traces which exhibit a width in the order 100's of meters (negative and positive relief) and esker ridges (width in the order of 10's of meters).

Proposed Classification	Description	Example
MW$_{Route}$	All traces of subglacial meltwater drainage (i.e. all of below)	
MW$_{Corridor}$	*'Negative':* - Meltwater Channel: - Tunnel channel - Tunnel valley - Hummock corridor (negative) (e.g. Peterson and Johnson, 2018; Lewington et al., 2019) - Erosional corridor (e.g. Burke et al., 2011) - Esker corridor (e.g. Sharpe et al., 2017) - Meltwater corridor (e.g. Rampton, 2000) - Washed zone (e.g. Ward et al., 1997) *'Positive':* - Glaciofluvial corridor (e.g. St-Onge, 1984; Utting et al., 2009) - Hummock corridor (positive) (e.g. Peterson and Johnson, 2018; Lewington et al., 2019) - Esker with splay (e.g. Cummings et al., 2011)	
Esker ridge	Single esker ridge	

535   While recognised previously in local case studies (e.g. St-Onge, 1984; Rampton, 2000; Utting et al., 2009), we confirm that across this 1 million km^2 area of the former LIS, MW$_{Corridors}$ of varying geomorphic expression are widespread rather than an isolated phenomenon. Within the study area, 87 % of all esker ridges were flanked by a MW$_{Corridor}$. Esker ridges alone were captured at just 6 % of our sample points while

540   a MW$_{Corridor}$ was recorded at 90 % (7 % of these were lateral splay, 21 % were meltwater channels and 73 % were meltwater tracks) - the remaining 4 % were coded as unclassified. However, we do note that the presence / absence of an esker at the sample point may not be indicative of the entire length of the MW$_{Route}$ as in many cases the esker ridge within a MW$_{Corridor}$ was fragmented. This suggests that the model of R-

545   channels across the Canadian Shield (e.g. Clark and Walder, 1994) is an oversimplification and the range of landforms observed suggests the presence of various modes of subglacial drainage varying between R-channels entirely cut up into the ice to those incised into the bed with a range in-between. Variations in form and pattern are likely to have been influenced by glaciological conditions, including ice

550   velocity, viscosity, temperature, and thickness, hydraulic potential gradient and water flux, and background conditions such as basal substrate, topography and local scale roughness.

5.1 A proposed model of formation: interaction of channelised and distributed
555   **drainage elements**

        To interpret palaeo-landforms and reconstruct subglacial meltwater behaviour an understanding of the processes that formed the landforms is needed (i.e. the 'glacial inversion' problem, e.g. Kleman and Borgström, 1996). One approach to
560   understanding glacial processes is through contemporary observations. In this section, we demonstrate how modern observations and modelling of the Variable Pressure Axis (VPA) around a subglacial conduit (e.g. Hubbard et al., 1995) is consistent with the form and distribution of mapped MW$_{Corridors}$ and can explain the range of depositional to erosional signatures observed in the study area.

565

        In steady-state conditions, conduits theoretically operate at a lower pressure than the surrounding high-pressure weakly connected system, and therefore will typically draw water in from their surroundings. However, variations in borehole water

pressure measurements observed beneath glaciers in the Alps (e.g. Hubbard et al.,
570   1995; Gordon et al., 1996) and Alaska (e.g. Bartholomaus et al., 2008), ice velocity
measurements taken from the Greenland Ice Sheet (e.g. Tedstone et al., 2014) and
numerical modelling (e.g. Werder et al., 2013), suggest that large and / or rapid
meltwater inputs can cause spikes in conduit water pressure (Cowton et al., 2013).
This temporarily reverses the hydraulic potential gradient and causes water to flow out
575   of the conduit and into the surrounding weakly-connected drainage system (Fig. 11).
This is because the conduit cross-sectional area cannot be expanded rapidly enough
by wall melt to accommodate high frequency (e.g. diurnal surface melt) and / or high
magnitude (e.g. supraglacial lake drainage) fluctuations in meltwater delivery. As
meltwater delivery to the conduit wanes or the conduit cross-sectional area grows at
580   a rate sufficient to accommodate the additional meltwater input, water pressure in the
conduit decreases and the conduit will again begin to capture water from its
surroundings. Hubbard et al., (1995) note that the pressure perturbation decreases
with lateral distance from the conduit like a dissipating wave across the VPA. The
distance either side of the conduit influenced by these variations (i.e. the width of the
585   VPA) appears variable over time and space, reaching a maximum of ~140 m in the
Alps (Hubbard et al., 1995; Gordon et al., 1996) and modelled to be ~2 km for the
western margin of the GrIS (Werder et al., 2013). This tallies well with the spectrum of
$MW_{Corridor}$ widths observed in this study, which range from ~100 m to > 3 km.
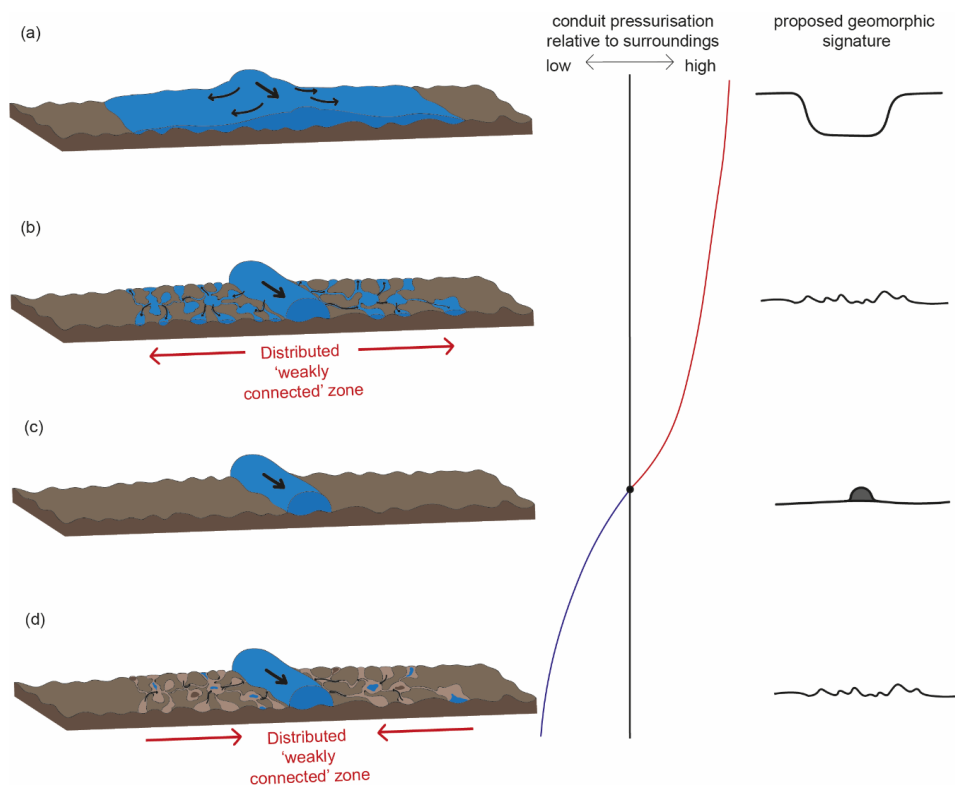
Figure 11. The interaction between a central conduit and the surrounding distributed 'weakly connected' zone with direction of water flow into and out of the conduit dependent on the variability and magnitude of discharge (Q). Water is forced out of the central conduit into the surrounding distributed system during periods of high Q (a-b) likely resulting in net erosion – and water and sediment flow back into the conduit during periods of low Q (d) – resulting in erosion or deposition of hummocks. Eskers are thought to be deposited in the conduit near the ice margin during the final stages of deglaciation.

Here, we propose that $MW_{Corridors}$ are the geomorphic signature of a VPA and represent the interaction between a conduit and the surrounding weakly connected system. Variations in $MW_{Corridor}$ expressions are hypothesised to occur due to variations in discharge and pressure (frequency, magnitude and duration) as well as

590

595

600

background glaciological, geological and topographical conditions, which together
605   determine the relative geomorphic activity (i.e. net erosion or deposition).

In this model, erosion of corridors with negative relief on the order of metres to
10s of metres depth is likely the result of large magnitude perturbations such as
supraglacial or subglacial lake drainages, with the rising limb of the flood event over-
610   pressurising the conduit and flooding the entire VPA (Fig. 11a). Flooding of this
broader VPA zone is analogous to a narrow sheet flood causing localised flotation or
hydraulic lifting (e.g. Brennand, 1994); similar processes have been recorded during
jökulhlaups in Iceland (e.g. Russell et al., 2007). Flow across the VPA would enhance
erosion by mobilising and entraining unconsolidated sediment in the high velocity flow
615   (e.g. Russell et al., 2006 and references within). As the flood event wanes, the
pressure perturbation is reversed causing water and sediment to flow back towards
the main conduit where it is rapidly evacuated. Less well defined features that have
experienced up to a few metres of erosion (i.e. those with more subdued relief and
less well defined boundaries) may be the result of repeated lower magnitude drainage
620   and pressure perturbations (e.g. from diurnal melt or rainfall) forcing water out across
the VPA. Instead of completely overwhelming and flooding the system, these events
may just fill and expand adjacent cavities (Fig. 11b). Delivery of water to the bed is
likely to occur at approximately the same location with lakes and crevasses 'locked'
into place by basal topography (e.g. Gudmundsson, 2003; Sergienko, 2013; Ignéczi
625   et al., 2018), resulting in repeated drainage down the same pathways. In this scenario,
the width of $MW_{Corridors}$ may represent a single maximum flow event or may represent
the lateral merging of multiple narrower flow events - as has been proposed for the
formation of some tunnel valleys (e.g. Jørgensen and Sandersen, 2006; Kehew et al.,
2012) – if the central conduit is positioned in a slightly different position across the bed
630   over time.

Sedimentological investigations suggest that hummocks within meltwater
tracks can occur as a result of erosion (e.g. Rampton, 2000) and / or deposition (e.g.
Utting et al., 2009) and our proposed model is able to explain each of these. Repeated
635   coupling / uncoupling of the ice-bed interface as water is forced in and out of the VPA
(Cowton et al., 2012) and subsequent erosion over seasons or longer may explain the
hummocky topography we see today (Fig. 4). Depositional hummocks may be formed

by a rapid increase in cross-sectional area associated with a breach in the conduit margin (i.e. it becomes unsealed) and flow across the VPA, facilitating rapid deposition within minor conduits and cavities (e.g. Brennand, 1994). When the conduit returns to being hydraulically isolated from the VPA following a decrease in water flow and pressure, standing bodies of water left within the cavities may also deposit minor fans which build up over time (Brennand, 1994). Alternatively, sediment may be trapped within cavities formed during turbulent sheet flow as water velocities subsequently decrease (Utting et al., 2009). Indeed, it is possible that lateral splays associated with esker ridges also formed due to conduit breaching and subsequent deposition, with outward fining in lateral fans suggesting conduit unsealing and decreasing hydraulic power (Cummings et al., 2011b). Finally, hummocks may be a combination of erosion and deposition. This is not dissimilar to the interpretation of triangular shaped landforms ('murtoos') which are thought to form from subglacial till transported by creep which is then eroded and shaped by subglacial meltwater, and represents high pressure distributed drainage within a 'weakly connected' zone upstream of channelised drainage (Mäkinen et al., 2017; Ojala et al., 2019).

Previous research indicates that esker ridges can be superimposed on hummocks within MW$_{Corridors}$ (e.g. Peterson et al., 2018), but to date, there are no examples of hummocks overlying eskers. Esker ridges do not always sit at the centre of their MW$_{Corridor}$ but instead meander across them, and are recorded alternately as left, central or right at different transect points. This is consistent with eskers being the final depositional imprint of channelised drainage within the large-scale MW$_{Routes}$ network, with formation close to the ice margin (e.g. Hebrand and Amark, 1989; Storrar et al., 2014b; Hewitt and Creyts, 2019; Livingstone et al., in review), while the corridors represent a composite imprint of drainage over a longer period.

5.2 A brief comment on possible alternative models

While we support the proposed model above, we acknowledge there are alternative formational mechanisms that can explain the wide meltwater tracks. In particular, it is possible that the width of meltwater tracks (i.e. an order of magnitude greater than the eskers commonly residing within them) is the consequence of a migrating conduit at the bed (Fig. 12). Within the study area, eskers are recorded at various positions across the meltwater tracks (i.e. not always at the centre) and are alternatively recorded as left or right aligned at various points down flow. To the best of our knowledge, there is no published research on the migration of contemporary conduits across ice sheet beds, although they may be expected to respond to variations in location or flow conditions by vertical and horizontal movement in a manner analogous to a central river within a floodplain. Therefore, it is possible that the meltwater corridor width is a result of a migrating central conduit.
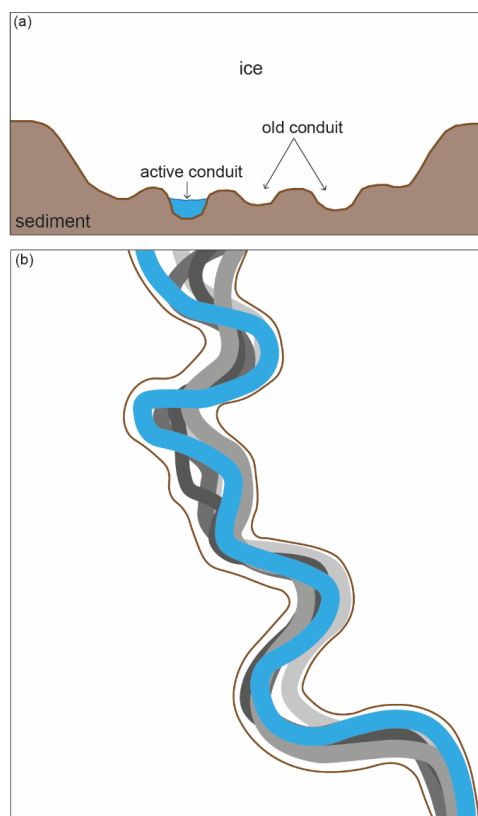
Figure 12. Schematic of alternative explanation of meltwater track width as a result of a migrating central conduit analogous to river migration across a flood plain in (a) cross sectional area and (b) plan in view.

5.3 Exploring potential controls on network patterns and variations in expression of MW$_{Routes}$

In this section, we explore spatial controls governing the overall pattern of the subglacial hydrologic network, as well as variations in meltwater landform expression (i.e. the balance between erosion / deposition and the resulting geomorphic

expression) along individual MW_{Routes}. Erosional and depositional features are frequently observed along the same MW_{Route} and even at the same location (e.g. eskers with lateral splay within wider meltwater channels (Fig. 4H)). This suggests that while spatial controls may be important and exert some control over the relative

710   'leakiness' of a conduit and therefore the resulting geomorphic signature at any location, there is also a temporal control. This is likely related to short-term variations in the magnitude and rate of subglacial meltwater delivery to the bed and the systems' ability to accommodate it.

715   We observe a high degree of channelisation across this sector of the ice sheet bed, but this is not uniform, with the densest areas of MW_{Routes} coinciding with the 'roughest' basal topography (Fig. 8). This may be the result of subglacial drainage route fragmentation around bed obstacles, with a greater number of tributaries and broken patterns common in regions of high bed roughness (e.g. Test Site 3). Basal

720   topography also preconditions the large-scale spatial structure of surface drainage (Ignéczi et al., 2018) and the association between rough areas and dense clusters of MW_{Routes} could be a response to more surface water penetrating to the bed as the result of extensive crevassing. In Greenland crevasses capture a significant amount of surface water – more than moulins or the hydrofracture of surface lakes (Koziol et

725   al., 2017). Surface meltwater inputs are thought to be an important control on the distribution of drainage across the bed (e.g. Gulley et al., 2012; Banwell et al., 2016) and the formation and evolution of subglacial meltwater landforms (e.g. Banerjee and McDonald, 1975; St-Onge, 1984; Hooke and Fastook, 2007; Storrar et al., 2014b; Livingstone et al., 2015; Peterson and Johnson, 2017).

730

Qualitatively, there are markedly fewer MW_{Routes} coinciding with palaeo-ice stream locations – particularly the Dubawnt Lake Ice Stream (Fig. 9). In addition, the network pattern of MW_{Routes} corresponding with the location of the Dubawnt Lake Ice Stream are more dendritic and extend further towards the ice divide. These observations are

735   consistent with Livingstone et al., (2015), who find fewer eskers on palaeo-ice stream beds where modelled subglacial meltwater drainage is greatest. We suggest the scarcity of MW_{Routes} beneath palaeo-ice streams is due to lower ice-surface slopes and hydraulic gradients, which favour distributed rather than channelised drainage (e.g. Kamb, 1987; Bell, 2008). Where channelised drainage does occur beneath palaeo-ice

740   streams, network patterns are typically more dendritic, which may also be the result of
shallower hydraulic gradients enabling greater lateral water flow.

Dynamic mass loss via streaming / surging has implications for ice sheet stability
(e.g. Bell, 2008; Christianson et al., 2014; Christoffersen et al., 2014). The Keewatin
745   sector of the LIS exhibits a relatively low frequency of ice streams (Margold et al.,
2015; Stokes et al., 2016). While this may be partially attributed to the resistant bed of
the shield (Clayton et al., 1985; Kamb, 1987; Stokes and Clark, 2003a, b), we also
suggest that efficient evacuation of meltwater through the dense channelised network
that developed in this region during the final stages of deglaciation, as the climate
750   warmed (Storrar et al., 2014b), would have inhibited the development of fast flow and
potentially contributed to the shut-down of existing ice streams (Lelandais et al., 2018).
This is consistent with modern observations that link decadal-scale ice-flow
decelerations with more pervasive and efficient drainage channelisation driven by
increased surface meltwater inputs to the bed (Sole et al., 2013; Tedstone et al., 2014;
755   van de Wal et al., 2015; Davison et al., 2019). We therefore hypothesise that this large-
scale inverse relationship between drainage channelisation and ice streaming will
exist in other palaeo-ice sheet settings. This potential drainage control on ice-sheet
activity may also influence the pace of deglaciation; we note slower retreat rates (~230
m yr^{-1}) in the northwest of the study area, which coincide with the highest density of
760   MW$_{Routes}$, compared to much faster retreat rates (~540 m yr^{-1}) associated with the
sparsest MW$_{Routes}$. This conclusion is tentative given uncertainty in the regions
deglacial chronology (Dyke et al., 2003) and requires further testing.

At a large-scale, there is a general tendency for MW$_{Routes}$ to form on till, which is
765   more easily eroded than bedrock and where geomorphic evidence is likely to be better
developed. Eskers are over-represented on harder, more resistant rock (Fig. 7d)
where R-channels are more likely to form (Clark and Walder, 1994; Storrar, 2014a),
while there is a slight tendency for meltwater channels (i.e. incisional features) to form
on the softer, more erodible sedimentary rock (Fig. 7b). Eskers with lateral splay (i.e.
770   depositional features) appear preferentially on till blankets (Fig. 7c) where there is an
abundance of sediment that may overwhelm and clog up the conduit (Burke et al.,
2015), while isolated esker ridges favour thin till and are under-represented on thick
till. Though detailed long-profiles (Fig. 10) hint at local relationships between bed

substrate changes and the resultant landform expression, we caution against the
775   assumption that this is a widespread occurrence rather than an isolated coincidence.

5.4 Relevance for understanding Greenland's hydrology and associated ice dynamic variations

780   Western sectors of the contemporary Greenland Ice Sheet are analogous to our
study area: both are underlain by resistant Precambrian Shield rocks and both
experience(d) rapid retreat and high meltwater production rates. This is also similar to
southern Sweden, which lay beneath the palaeo Scandinavian Ice Sheet, where
similar geomorphic features to those described here, occur extensively (e.g. Peterson
785   et al., 2017; Peterson and Johnson, 2017). This study therefore has potential
implications for our understanding of the impact of subglacial hydrology on overlying
ice dynamics and ice flow regulation of past, current and future ice sheets.

The interaction between a subglacial conduit and the surrounding weakly-
790   connected drainage system (VPA) is believed to be widespread in contemporary
glaciological settings (e.g. Hubbard et al., 1995; Gordon et al., 1996; Bartholomaus et
al., 2008; Werder et al., 2013; Tedstone et al., 2014) and has been identified as key
to understanding ice velocity variations and predicting future ice sheet mass loss
(Davison et al., 2019). However, the true extent and influence of VPAs beneath the
795   Greenland Ice Sheet is unknown due to the challenge of observing contemporary
subglacial environments. Palaeo-studies, such as this one, offer the potential to reveal
new insights into the nature and configuration of the subglacial hydrological system at
an ice sheet scale.

800   Based on our proposed model and the observations within this study we suggest
that the VPA is widespread across the Keewatin sector of the LIS, which may be
analogous to parts of western Greenland. The drainage footprint is considerably more
dense if we consider $MW_{Corridors}$ as well as esker ridges as indicators of areas of the
bed which were influenced by subglacial meltwater. The drainage footprint in our study
805   is estimated to cover ~13 % of the bed (using average width and spacing of MW_{Routes})
but could realistically vary between 5 % (lower quartile width and upper quartile
spacing) and 36 % (upper quartile width and lower quartile spacing) if we assume that

MW$_{Routes}$ were active at the same time. This represents an area 25 times greater than that of eskers alone which cover ~0.5 % of the bed (using average esker width (100 m) and spacing (18.8 km; Storrar et al., 2014b). The dynamic influence is likely to extend even further beyond the VPA due to lateral stress transfer within the ice (Tedstone et al., 2014). In the longer term, increased channelisation may have additional ice dynamic implications; effectively removing large volumes of meltwater and reducing ice velocity, potentially limiting dynamic mass loss via streaming / surging (e.g. Storrar et al., 2014b).
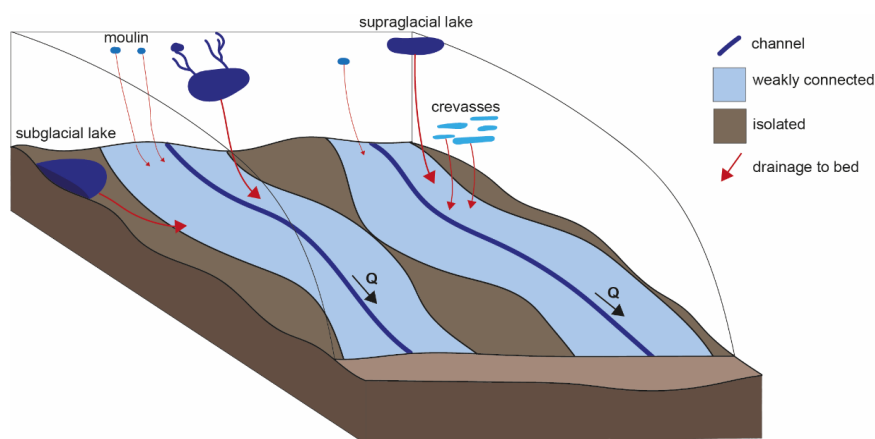
Figure 13. Schematic of the VPA (light blue) beneath a contemporary ice sheet with inputs from the surface and the bed influencing discharge (Q) and therefore the VPA.

6. Conclusions

We identified and mapped all visible traces of subglacial meltwater drainage in the Keewatin sector of the former LIS. We found that wider meltwater features (meltwater tracks, meltwater channels and eskers with lateral splays on the order of 100s to 1000s m) flanking or joining up intervening segments of esker ridges were common. These have previously been termed and described as different features. However, owing to similarities in spacing, morphometry and spatial location (i.e. part of the same

integrated network), we propose collectively grouping these features under the term MW$_{Corridor}$ (table 2). Combing multiple features within a single MW$_{Routes}$ map (i.e. esker ridges and all varying geomorphic expressions of MW$_{Corridors}$), we have created the first large-scale holistic map of subglacial meltwater drainage.

Based on our observations and modern analogues, we propose a new model which accounts for the formation and geomorphic variations of MW$_{Corridors}$. In this model, we propose that a central conduit (i.e. the esker) interacts with the surrounding distributed drainage network or VPA (i.e. the MW$_{Corridor}$) with the relative extent / intensity of this interaction, determined by the magnitude and rate of meltwater delivery to the subglacial conduit and the resulting water pressure variability. Controls governing the geomorphic expression of the VPA, such as net erosion or deposition, is likely a combination of glaciological (i.e. relative water pressure fluctuation) and background controls (i.e. topography, basal substrate). Eskers likely represent the final depositional imprint of channelised drainage within the large-scale MW$_{Routes}$ network, with formation close to the ice margin, while the corridors represent a composite imprint of drainage over a longer time period. If our model is correct, incorporating the width of the VPA (i.e. the 'weakly connected' drainage system), the drainage footprint in this sector of the ice sheet covered 5–36 % of the bed (on average), which is 25 times greater than previously assumed from esker studies alone, which only account for the central conduit.

Our results suggest that the overall distribution and pattern of drainage is influenced by background topography, with greater relief resulting in denser channelised networks, possibly due to fragmentation of subglacial drainage around basal obstacles and / or enhanced meltwater delivery to the bed through crevasses. Channelised drainage is relatively rare beneath palaeo ice streams, which may favour distributed drainage configurations due to the lower ice surface slopes and hydraulic gradients. Meltwater drainage may also influence ice dynamics, with the high degree of channelisation observed in the region able to efficiently dewater the bed causing ice-flow deceleration and limiting ice stream activity.

Further research should focus on determining how common this proposed interaction between conduits and the surrounding distributed drainage system is

beneath other palaeo and contemporary ice sheets and the controls governing its variability. We hypothesise that where less surface meltwater is delivered to the bed or ice-surface slopes are shallower, for instance, when the LIS was larger and the climate colder, the geomorphic expression will be less extensive and fainter. This is

870   because conduits are less likely to evolve due to lower hydraulic gradients, and their interaction with the surrounding distributed system reduced because of invariant melt supply. Understanding where this interaction and signature occurs will help confirm or refute our proposed model, and develop understanding of how meltwater drainage evolves over long time-scales and influences ice dynamics and mass balance.

875

7. Acknowledgements

This work was funded through: "Adapting to the Challenges of a Changing

880   Environment" (ACCE); a NERC funded doctoral training partnership ACCE DTP (NE/L002450/1). This work also benefitted from the PALGLAC team of researchers who received funding from the European Research Council (ERC) under the European Union's Horizon 2020 research and innovation programme (Grant agreement No. 787263). DEMs were provided by the Polar Geospatial centre under

885   NSF-OPP awards 1043681, 1559691, and 1542736.

8. References

890   Andrews, L.C. Catania, G.A. Hoffman, M.J. Gulley, J.D. Lüthi, M.P. Ryser, C. et al., Direct observations of evolving subglacial drainage beneath the Greenland Ice Sheet. Nature, 514(7520). 80–83. 2014

Aylsworth, J. M. and Shilts, W. W. Glacial features around the Keewatin Ice Divide: Districts of
895   Mackenzie and Keewatin. Geological Survey of Canada, Map 24-1987. 1:1,000,000. 1989.

Aylsworth, J.M. Shilts, W.W. Russel, H.A.J. Pyne, D.M. Eskers around the Keewatin Ice Divide: Northwest Territories and Nunavut. Geological Survey of Canada, Open File, 7047. 2012.

900   Banerjee, I. McDonald, B.C. Nature of esker sedimentation. In: Jopling, A.V. McDonald, B.C. (Eds.), Glaciofluvial and Glaciolacustrine Sedimentation, vol 23. Society of Economic Palaeonologists and Mineralogists. Special Publication. 304-20. 1975.

905   Banwell, A.D. Arnold, N.S. Willis, I.C. Tedesco, M. Ahlstrøm, A.P. Modelling supraglacial water
            routing and lake filling on the Greenland Ice Sheet. J. Geophys. Res. 117. 2012.

        Banwell, A. Hewitt, I. Willis, I. Arnold, A. Moulin density controls drainage development beneath
            the Greenland ice sheet. Journal of Geophysical Research: Earth Surface. 121: 2248-69.
            2016.
910

        Bartholomaus, T.C., Anderson, R.S. Anderson, S.P. Response of glacier basal motion to transient
            water storage. Nature Geoscience, 1. 33–37. 2008.

        Bell, R.E. The role of subglacial water in ice-sheet mass balance. Nat. Geosci. 1(5): 297-304. 2008.
915

        Bindscahlder, R.A. The importance of pressurized subglacial water in seperation and sliding at the
            glacier bed. Journal of Glaciology. 57: 929-41. 1983.

        Bingham, R.G. Hubbard, A.L. Nienow, P.W. Sharp, M.J. An investigation into the mechanisms
920   controlling seasonal speedup events at a High Arctic glacier. Journal of Geophysical
            Research. 113. 2008.

        Bolduc, A.M. The formation of eskers based on their morphology, stratigraphy and lithologic
            composition, Labrador, Canada (Unpublished Ph.D thesis). Lehigh University. 1992.
925

        Boulton, G. S., Caban, P. E. and Van Gijssel, K. Groundwater flow beneath ice sheets: part I -
            large scale patterns. Quaternary Science Reviews, 14, 545-562. 1995.

        Boulton, G.S. Lunn, R. Vidstrand, P. Zatspein, S. Subglacial drainage by groundwater-channel
930   coupling, and the origin of esker systems: Part I – Glaciological observaations. Quaternary
            Science Reviews. 26(7–8). 1067-90. 2007a.

        Boulton, G.S. Lunn, R. Vidstrand, P. Zatspein, S. Subglacial drainage by groundwater-channel
            coupling, and the origin of esker systems: Part II - Theory and simulation of a modern
935   system. Quaternary Science Reviews. 26(7–8). 1091–105. 2007b.

        Boulton, G. S., Hagdorn, M., Maillot, P. B. and Zatsepin, S. Drainage beneath ice sheets:
            groundwater-channel coupling, and the origin of esker systems from former ice sheets.
            Quaternary Science Reviews, 28, 621-638. 2009.
940

        Boulton, G.S. Hindmarsh, R.C.A. Sediment deformation beneath glaciers: rheology and geological
            consequences. Journal of Geophysical Research. 92. 9059-82. 1987.

        Brennand, T.A. Deglacial meltwater drainage and glaciodynamics: Inferences from Laurentide
945   eskers, Canada. Geomorphology. 32(3–4). 263–93. 2000.

        Brennand, T.A. Shaw, J. Tunnel channels and associated landforms, south-central Ontario: their
            implication for ice-sheet hydrology. Canadian Journal of Earth Sciences. 31. 505-22. 1994.

950   Burke, M.J. Brennand, T.A. Perkins, A.J. Evolution of the subglacial hydrologic system beneath
            the rapidly decaying Cordilleran Ice Sheet by ice-dammed lake drainage: implications for
            meltwater-induced ice acceleration. Quaternary Science Reviews. 50: 125-40. 2012.

955   Burke, M.J. Brennand, T.A. Sjogren, D.B. The role of sediment supply in esker formation and ice tunnel evolution. Quaternary Science Reviews. 115: 50-77. 2015.

Carlson, A.E. Legrande, A.N. Oppo, D.W. Came, R.E. Schmidt, G.A. Anslow, F.S. Licciardi, J.M. Obbink, E.A. Rapid early Holocene deglaciatin of the Laurentide ice sheet. Nature Geoscience. 1(9): 620-24. 2008.

960   Carlson, A.E. Anslow, F.S. Obbink, E.A. LeGrande, A.N. Ullman, D.J. Licciardi, J.M. Surface melt driven Laurentide Ice Sheet retreat during the early Holocene. Geophysical Research Letters. 36. 2009.

965   Chandler, B. M. P., Lovell, H., Boston, C. M., Lukas, S., Barr, I. D., Benn, D. I., Clark, C. D., Darvill, C. M., Evans, D. J. A., Ewertowski, M., Loibl, D., Margold, M., Otto, J., Roberts, D. H., Stokes, C. R., Storrar, R. D. and Stroeven, A. Glacial geomorphological mapping: a review of approaches and frameworks for best practice. Earth-Science Reviews, 185, 806-846. 2018.

970   Christianson, K. Peters, L.W. Alley, R.B. Anandakrishnan, S. Jacobel, R.W. Riversman, K.W. Muto, A. Keisling, B.A. Dilatant till facilitates ice-stream flow in northeast Greenland. Earth Planet. Sci. Lett. 401: 57-69. 2014.

975   Christoffersen, P. Bougamont, M. Carter, S.P. Fricker, H.A. Tulaczyk, S. Significant groundwater contribution to Antarctic streams hydrologic budget. Geophysical Research Letters. 41. 2003-10. 2014.

980   Clark, P.U. Walder, J.S. Subglacial drainage, eskers, and deforming beds beneath the Laurentide and Eurasian ice sheets. Geol. Soc. Am. Bull. 106: 304 – 14. 1994.

Clayton, L. Teller, J.T. Attig, J.W. Surging of the southwestern part of the Laurentide ice sheet. Boreas. 14: 235-41. 1985.

985   Cowton, T. Nienow, P. Sole, A. Wadham, J. Lis, G. Bartholomew, I. et al., Evolution of drainage system morphology at a land-terminating Greenlandic outlet glacier. Journal of Geophysical Research. Earth Surface Processes. 118. 29-41. 2013.

990   Cowton, T. Nienow, P. Bartholomew, I. Sole, A. Mair, D. Rapid erosion beneath the Greelnad ice sheet. Geology. 40: 343:46. 2012.

Cummings, D.I. Kjarsgaard, B.A. Russell, H.A.J. Sharpe, D.R. Eskers as mineral exploration tools. Earth Science Reviews. 109: 32-43. 2011a.

995   Cummings, D.I. Gorrell, G. Guillbault, J-P. Hunter, J.A. Logan, C. Ponomarenko, D. Pugin. A. J-M. Pullan, S.E. Russell, H.A.J. Sharpe, D.R. Sequence stratigraphy of a glaciated basin fill, with a focus on esker sedimentation. Geological Society of American Bulletin. 2011b.

1000   Cutler, P.M. Colgan, P.M. Mickelson, D.M. Sedimentological evidence for outburst floods from the Laurentide Ice Sheet margin in Wisonsin, USA: implications for tunnel-channel formation. Quaternary Internationl. 90. 23-40. 2002.

1005   Das, S.B. Joughin, I. Behn, M.D. Howat, I.M. King, M.A. Lizarralde, D. Bhatia, M.P. Fracture propagation to the base of the Greenland Ice Sheet during supraglacial lake drainage. Science. 320 (5877). 963-64. 2008.

Davison, B.J. Sole, A.J. Livingstone, S.J. Cowton, T.W. Nienow, P.W. The influence of hydrology on the dynamics of land-terminating sectors of the Greenland Ice Sheet. Front. Earth Sci. 7:10. 2019.

1010

Doyle, S.H. Hubbard, A. Fitzpatrick, A.A.W. van As, D. Mikkelsen, A.B. Pettersson, R. et al., Persistant flow acceleration within the interior of the Greenland ice sheet. Geophysical Research Letters. 41: 899-905. 2014.

1015   Doyle, S.H. Hubbard, A. Van De Wal, R.S. van As, D. Scharrer, K. Meierbachtol, T.W. et al., Amplified melt and flow of the Greenland ice sheet driven by late-summer cyclonic rainfall. Nature Geoscience. 8: 647-53. 2015.

Dredge, L. Nixon, F. Richardson, R. Surficial Geology, Northwestern Manitoba: Geological Survey of Canada, 'A' Series Map 1608A, 1: 500 000. 1985.

1020

Dyke, A.S. Moore, A. Robertson, I. Deglaciation of North America. Geological Survey of Canada. Open File, 1574. 2003.

1025   Englehardt, H. Harrison, W. Kamb, B. Basal sliding and conditions at the glacier bed as revealed by bore-hole photography. Journal of Glaciology. 20: 469-508. 1978.

Fitzpatrick, A.A. Hubbard, A. Joughin, I. Quincey, D.J. Van As, D. Mikkelsen, A.P. et al., Ice flow dynamics and surface meltwater flux at a land-terminating sector of the Greenland ice sheet. Journal of Glaciology. 59: 687-96. 2013.

1030

Fowler, A. Sliding with cavity formation. Journal of Glaciology. 33: 131-41. 1987.

Fulton, R.J. Surficial materials of Canada. Geological Survey of Canada, 'A' Series Map 1880A. 1:5,000,000. 1995.

1035

Gordon, S. Sharp, M. Hubbard, B. Smart, C. Ketterling, B. Willis, I. Seasonal reorganization of subglacial drainage inferred from measurements in boreholes. Hydrological Processes. 12. 105-33. 1998.

1040

Gorrell, G. Shaw, J. Deposition in an esker, bead and fan complex, Lanark, Ontario, Canada. Sedimentary Geology. 72(3-4): 285-314. 1991.

Greenwood, S.L. Clark, C.D. The sensitivity of subglacial bedform size and distribution to substrate lithological control. Sedimentary Geology. 232: 130-44. 2010.

1045

Glasser, N.F. Sambrook Smith, G.H. Glacial meltwater erosion of the Mid-Cheshire Ridge: implications for ice dynamics during the Late Devensian glaciation of northwest England. Journal of Quaternary Science. 14: 703-10. 1999.

1050

Gudmundsson, G.H. Transmission of basal variability to a glacier surface. Journal of Geophysical Research: Solid Earth. 108(B5). 2003.

1055   Gulley, J.D. Grabiec, M. Martin, J.B. Jania, J. Catania, G. Glowacki, P. The effect of discrete
       recharge by moulins and heterogenity in flow-path efficiency at glacier beds on subglacial
       hydrology. Journal of Glaciology. 58(211). 2012.

       Hebrand, M. Amark, M. Esker formation and glacier dynamics in eastern Skane and adjacecnt
       areas, southern Sweden. Boreas. 18(1): 67-81. 1989.
1060

       Hewitt, I.J. Modelling distributed and channelized subglacial drainage: the spacing of channels.
       Journal of Glaciology. 57(202). 2011.

       Hewitt, I.H. Creyts, T.T. A model for the formation of eskers. Geophysical Research Letters. 46.
1065   2019.

       Hodge, S.M. Direct measurements of basal water pressures: progress and problems. Journal of
       Glaciology. 23, 309-19. 1979.

1070   Hoffman, M.J. Andrews, L.C. Price, S.A. Catania, G.A. Neumann, T.A. Luthi, M.P. et al., Greenland
       subglacial drainage evolution regulated by weakly connected regions of the bed. Nature
       Communications. 7: 13903. 2016.

       Hooke, R.L. Fastook, J. Thermal conditions at the bed of the Laurentide ice sheet during
1075   deglaciation: implications for esker formation. Journal of Glaciology. 53(183). 2006.

       Hooke, R.L. Jennings, C.E. On the formation of the tunnel valleys of the southern Laurentide ice
       sheet. Quaternary Science Reviews. 25(11–12). 1364–72. 2006.

1080   Hooke, R. LeB. Laumann, T. Kohler, J. Subglacial water pressures and the shape of subglacial
       conduits. Journal of Glaciology. 36 (122). 67-71. 1990.

       Hoyal, D.C.J.D. Van Wagoner, J.C. Adair, N.L. Deffenbaugh, M. Li, D. Sun, T. Huh, C. Griffin, D.E.
       Sedimentation from jets: A depositional model for clastic deposits of all scales and
1085   environments: Salt Lake City, Utah, Search and Discovery Article No. 40082, American
       Association of Petroleum Geologists Annual Meeting, May 14, 2003, 10.

       Hubbard, B.P. Sharp, M.J. Willis, I.C. Nielsen, M.K. Smart, C.C. Borehole water-level variation and
       the structure of the subglacial hydrological system of Haut Glacier d'Arolla, Valais,
1090   Switzerland. Journal of Glaciology. 41(139). 572–83. 1995.

       Ignéczi, A. Sole, A.J. Livingstone, S.J. Ng, F.S.L. Yang, K. Greenland ice sheet surface topography
       and draiange structure controlled by transfer of basal variability. Frontiers in Earth Science.
       6: 101. 2018.
1095

       Iken, A. Bindschadler, R.A. Combined measurements of subglacial water pressure and surface
       velocity of Findelengletscher, Switzerland: conclusions about drainage system and sliding
       mechanisms. Journal of Glaciology. 32: 101-19. 1986.

1100   Iken, A. Rothlisberger, H. Flotron, A. Harberli, W. The uplift of Unteraargletscher at the beginning
       of the melt season – a consequence of water sorage at the bed? Journal of Glaciology. 29:
       28-47. 1983.

1105 Iverson, N.R. Baker, R.W. Hooke, R.L. Hanson, B. Jansson, P. Coupling between a glacier and a
        soft bed: I. A relation between effective pressure and local shear stress determined from
        till elasticity. Journal of Glaciology. 45: 31-40. 1999.

      Jørgensen, F. Sandersen, P.B.E. Buried and open tunnel valleys in Denmark – erosion beneath
        multiple ice sheets. Quaternary Science Reviews. 25(11-12): 1339-63. 2006.

1110
      Joughin, I. Das, S.B. King, M. Smith, B.E. Howat, I.M. Moon, T. Seasonal speedup along the
        western flank of the Greenland Ice Sheet. Science. 320: 781-83. 2008.

      Kamb, B. Glacier surge mechanism based on linked cavity configuration of the basal water conduit
1115   system. Journal of Geophysical Research, Solid Earth. 92(B9). 9038-100. 1987.

      Kamb, B. Raymond, C. Harrison, W. Engelhardt, H. Echelmeyer, K. Humphrey, N. et al., Glacier
        surge mechanism: 1982-1983 surge of Variegated Glacier, Alaska. Science. 227: 469-79.
        1985.

1120
      Kehew, A.E. Nicks, L.P. Straw, W.T. Palimpsest tunnel valleys: evidence for relative timing of
        advances in an interlobate area of the Laurentide ice sheet. Ann. Glaciol. 28: 47 – 52.
        1999.

1125 Kehew, A.E., Piotrowski, J.A. and Jørgensen, F. Tunnel valleys: Concepts and controversies - A
        review. Earth-Science Reviews. 113(1–2). .33–58. 2012.

      Kleman, J. Borgström, I. Reconstruction of palaeo-ice sheets: the use of geomorphological data.
        Eart Surface Processes and Landforms. 21(10): 893-909. 1996.

1130
      Koziol, C. Arbold, A. Pope, A. Colgan, W. Uantifying supraglacil meltwater pathways in the
        Paakitsoq region, West Greenland. Journal of Glaciology. 63(239): 464-76. 2017.

      Kerr, D. Knight, R. Sharpe, D. Cummings, D. Reconnaissance surficial geology, Lynx Lake,
1135   Northwest Territories, NTS 75-J: Geological Survey of Canada, 1: 125 000. 2014a.

      Kerr, D. Knight, R. Sharpe, D. Cummings, D. Reconnaissance surficial geology, Walmsley Lake,
        Northwest Territories, NTS 75-N, Canadian Geoscience Map-140: Geological Survey of
        Canada, 1:125 000. 2014b.

1140
      Lee, H.A. Craig, B.G. Fyles, J.G. Keewatin ice divide. Geol. Soc. Am. Bull. 68: 1760-61. 1957.

      Lelandais, T. Ravier, E. Pochat, S. Bourgeois, O. Clark, C. Mourgues, R. Strzerzynski, P. Modelled
        subglacial floods and tunnel valleys control the life cycle of transitory ice streams. The
1145   Cryosphere. 12: 2759-72. 2018.

      Lewington, E.L.M. Livingstone, S. Sole, A.J. Clark, C.D. Ng, F. An automated method for mapping
        geomorphological expressions of former subglacial meltwater pathways (hummock
        corridors) from high resolution digital elevation data. Geomorphology. 339: 70-86. 2019.
1150

Livingstone, S.J. and Clark, C.D. Morphological properties of tunnel valleys of the southern sector of the Laurentide ice sheet and implications for their formation. Earth Surface Dynamics. 4. 567–89. 2016.

1155 Livingstone, S.J Storrar, R.D. Hillier, J.K. Stokes, C.R. Tarasov, L. An ice-sheet scale comparison of eskers with modelled subglacial drainage routes. Geomorphology. 246. 104–12. 2015.

Livingstone, S.J. Lewington, E.L.M. Clark, C.D. Storrar, R.D. Sole, A.J. McMartin, I. Dewald, N. Ng, F.. A quasi-annual record of time-transgressive esker formation: implications for ice
1160 sheet reconstruction and subglacial hydrology. The Cryosphere Discuss. In review, 2019.

Lliboutry, L. General theory of subglacial cavitation and sliding of temperate glaciers. Journal of Glaciology. 7. 21-58. 1968.

1165 Mäkinen, J. Time-transgressive deposits of repeated depositional sequences within interlobate glaciofluvial (esker) sediments in Köyliö, SW Finalnd. Sedimentology 50. (2): 337-60. 2003.

Mäkinen, J. Kajutti, K. Palmu, J-P. Ojala, A. Ahokangas, E. Triangular-shaped landforms reveal subglacial drainage routes in SW Finland. Quaternary Science Reviews. 164. 37–53. 2017.
1170
Margold, M. Stokes, C.R. Clark, C.D. Ice streams in the Laurentide Ice Sheet: Identification, characteristics and comparison to modern ice sheets. Earth Science Reviews. 143. 117-46. 2015.

1175 Margold, M. Stokes, C.R. Clark, C.D. Reconciling records of ice streaming and ice margin retreat to produce a palaeographic reconstruction of the deglaciation of the Laurentide Ice Sheet. Quaternary Science Reviews. 189: 1-30. 2018.

McMartin, I. Henderson, P. J. Evidence from Keewatin (central Nunavut) for paleo-ice divide
1180 migration. Géographie physique et Quaternaire, 58, 163-186. 2004.

Mooers, H.D. On the formation of the tunnel valleys of the Superior Lobe, Central Minnesota. Quaternary Research. 32: 24 – 35. 1989.

1185 Ng, F. Ignéczi, A. Sole, A.J. Livingstone, S.J. Response of surface topography to basal variability along glacial flowlines. Journal of Geophysical Research: Earth Surface. 123: 2319-40. 2018.

Nienow, P. Sharp, M. Willis, I. Seasonal changes in the morphology of the subglacial drainage
1190 system, Haut Glacier d'Arolla, Switzerland. Earth Surface Processes and Landforms. 23: 825-84. 1998.

Noh, M.J. Howat, I.M. Automated stereo-photogrammetric DEM generation at high lattitudes: Surface Extraction with TIN-based Search-space Minimisation (SETSM) validation and
1195 demonstration over glaciated regions. GISci. Remote Sens. 52(2), 198-217. 2015.

Nye, J. Water at the bed of a glacier. IASH Publications 95. (Symposium at Cambridge 1969 – Hydrology of Glaciers). Pp. 189-194. 1973.

1200 Ó Cofaigh, C. Tunnel valley genesis. Progress in Physical Geography. 20. 1-19. 1996.

Ojala, A.E.K. Peterson, G. Mäkinen, J. Johnson, M.D. Kajutti, K. Palmu, J-P. Ahokangas, E. Öhrling, C. Ice-sheet scale distribution and morphometry of triangular shaped hummocks (murtoos): a subglacial landform produced during rapid retreat of the Scandinavian Ice Sheet. Anals of Glaciology. 1-12. 2019.

Palmer, S. Shepherd, A. Nienow, P. Joughin, I. Seasonal speed-up of the Greenland ice sheet linked to routing of surface water. Earth Planet Science Letters. 302: 423-28. 2011.

Perkins, A.J., Brennand, T.A. Burke, M.J. Towards a morphogenetic classification of eskers: Implications for modelling ice sheet hydrology. Quaternary Science Reviews. 134. 19–38. 2016.

Peterson, G. Johnson, M.D. Hummock corridors in the south-central sector of the Fennoscandian ice sheet, morphometry and pattern. Earth Surface Processes and Landforms. 43: 919-29. 2018.

Peterson, G. Johnson, M.D. Smith, C.A. Glacial geomorphology of the south swedish uplands – focus on the spatial distribution of hummock tracts. Journal of Maps. 13(2): 534 – 44. 2017.

Peterson, G. Johnson, M.D. Dahlgren, S. Passe, T. Alexanderson, H. Genesis of hummocks found in tunnel valleys: an example from Horda, southern Sweden. GFF. 140(2): 189 – 544. 2018.

Piotrowski, J.A. Tunnel-valley formation in north west Germany – geology, mechanisms of formation and subglacial bed conditions for the Bornhoved tunnel valley. Sedimentary Geology. 89. 107-41. 1994.

Piotrowski, J.A. Channelized subglacial drainage under soft-bedded ice sheets: evidence from small N-channels in Central European lowland. Geol. Q. 43(2): 153-62. 1999.

Porter, C., Morin, P., Howat, I., Noh, M.J., Bates, B., Peterman, K., Keesey, S., Schlenk, M., Gardiner, J., Tomko, K. Willis, M., et al., ArcticDEM. Harvard Dataverse, V1. 2018.

Powell, R.D. Glacimarine processes at grounding-line fans and their growth to ice-contact deltas. Geological Society, London, Special Publications, 53(1): 53-73. 1990.

Praeg, D. Seismic imaging of mid-Pleistocene tunnel valleys in the North Sea Basin – high resolution from low frequencies. Journal of Applied Geophysics. 53 273-298. 2003.

Prowse, N.D. Morphology and Sedimentology of Eskers in the Lac de Gras Area, Northwest Territories, Canada. PhD Thesis. Carleton University. Ottawa, Canada. 2017.

Price, S.F. Payne, A.J. Catania, G.A. Neumann, T.A. Seasonal acceleration of inland ice via longitudinal coupling to marginal ice. Journal of Glaciology. 54: 213-19. 2008.

Punkari, M. Glacial and glaciofluvial deposits in the interlobate areas of the Scandinavian Ice Sheet. Quaternary Science Reviews, 16, 741-753. 1997.

1250   Rampton, V.N. Large-scale effects of subglacial meltwater flow in the southern Slave Province,
                Northwest Territories, Canada. Canadian Journal of Earth Sciences. 37(1). 81–93. 2000.

        Rothlisberger, H. Water pressure in Intra-and Subglacial Channels. Journal of Glaciology. 11: 177-
                203. 1972.
1255
        Russell, A.J., Gregory, A.R., Large, A.R., Fleisher, P.J. and Harris, T.D. Tunnel channel formation
                during the November 1996 jökulhlaup, Skeiðarárjökull, Iceland. Annals of Glaciology, 45,
                95-103. 2007.

1260   Russell, A.J. Roberts, M.J. Fay, H. Marren, P.M. Cassidy, N.J. Tweed, F.S. Harris, T. Icelandic
                jökulhlaups impacts: Implications for ice-sheet hydrology, sediment transfer and
                geomorphology. Geomorphology. 75: 33-64. 2006.

        Rust, B.R. Romanelli, R. Late quaternary subaqueous outwash deposits near Ottawa, Canada.
1265   A.V. Jopling, B.C. McDonald (Eds.), Glaciofluvial and Glaciolacustrine Sedimentation, Soc.
                Econ. Paleontol. Mineral., Spec. Publ. 177-92. 1975.

        Sergienko, O. V. Glaciological twins: Basally controlled subglacial and supraglacial lakes. Journal
                of Glaciology. 59(213). 3–8. 2013.
1270
        Sharpe, D., Kjarsgaard, B. Knight, R.D. Russell, H.A.J. Kerr, D.E. Glacial dispersal and flow
                history, East Arm area of Great Slave Lake, NWT, Canada. Quaternary Science Review.
                165: 49 – 72. 2017.

1275   Shepherd, A. Hubbard, A. Nienow, P. King, M. McMillan, M. Joughin, I. Greenland ice sheet motion
                coupled with daily melting in lare summer. Geophysical Research Letters. 36: 2-5. 2009.

        Shilts, W.W. Aylsworth, J.M. Kaszycki, C.A. Klasson, R.A. Canadian Shield. In: Graf, W.L. (Ed.),
                Geomorphi Systems of North America. Geological Society of America, Boulder, Colorado.
1280   pp. 119-61. Centennial Special Volume 2. 1987.

        Shreve, R.L. Movement of water in glaciers. Journal of Glaciology. 11(62). 205–14. 1972.

        Shreve, R.L. Esker characteristics in terms of glacial physics, Katahdin esker system, Maine. Geol.
1285   Soc. Am. Bull. 96, 639 – 46. 1985.

        Sissons, J.B. A subglacail drainage system by the Tinto Hills, Lankashire. Trans Edinb. Geol. Soc.
                18: 175 – 92. 1961.

1290   Sjogren, D.B. Fisher, T.G. Taylor, L.D. Jol, H.M. Munro-Stasiuk, M.J. Incipient tunnel channels.
                Quaternary International. 90. 41–56. 2002.

        Smith, M.J. Clark, C.D. Methods for the cisualisation of digital elevation models for landform
                mapping. Earth Surface Processes and Landforms. 30(7) : 885-900. 2005.
1295
        Sole, A. Nienow, P. Bartholomew, I. Mair, D. Cowton, T. Tedstone, A. et al., Winter motion
                mediates dynamic response of the Greenland Ice Sheet to warmer summers. Geophysical
                Research Letters. 40(15). 3940–44. 2013.

1300   Stevens, L.A. Behn, M.D. Das, S.B. Joughin, I. Noel, B.P. Broeke, M.R. et al., Greenland Ice Sheet
flow response to runoff variability. Geophys. Res. Lett. 43: 11295-303. 2016.

Stokes, C.R. Clark, C.D. TheDubawnt Lake palaeo-ice stream: evidence for dynamic ice sheet
behaviour on the Canadian Shield and insights regarding the controls on ice-stream
1305   location and vigour. Boreas. 32(1): 263-79. 2003a.

Stokes, C.R. Clark, C.D. Laurentide ice streaming on the Canadian Shield: A conflict with the soft-
bedded ice stream paradigm? Geology. 31(4): 347-50. 2003b.

1310   Stokes, C. R., Margold, M., Clark, C. D. Tarasov, L. Ice stream activity scaled to ice sheet volume
during Laurentide Ice Sheet deglaciation. Nature, 530: 322-326. 2016.

St-Onge, D.A. Surficial deposits of the Redrock Lake area, District of Mackenzie; in Current
Research, Part A, Geological Survey of Canada, Paper 84 (1A). 271-78. 1984.
1315
Storrar, R.D. Reconstructing subglacail meltwater dynamics from the spatial and temporal variation
in the form and pattern of eskers. Doctoral thesis, Durham University. 2014.

Storrar, R. D., Ewertowski, M., Tomczyk, A., Barr, I. D., Livingstone, S. J., Ruffell, A., Stoker, B.
1320   Evans, D. J. A. Equifinality and preservation potential of complex eskers. Boreas. 2019.

Storrar, R.D. Livingstone, S.J. Glacial geomorphology of the northern Kivalliq region, Nunavut,
Canada, with an emphasis on meltwater drainage systems. J. Maps. 13: 153-64. 2017.

1325   Storrar, R.D. Stokes, C.R. Evans, D.J.A. A map of large Canadian eskers from Landsat imagery.
Journal of Maps. 3: 456-73. 2013.

Storrar, R.D. Stokes, C.R. Evans, D.J.A. Morphometry and pattern of a large sample (> 20,000) of
Canadian eskers and implications for subglacial drainage beneath ice sheets. Quaternary
1330   Science Reviews. 105: 1 – 25. 2014a.

Storrar, R.D., Stokes, C.R. Evans, D.J.A. Increased channelization of subglacial drainage during
deglaciation of the Laurentide Ice Sheet. Geology. 42(3). 239–42. 2014b.

1335   Stroeven, A. P., Hättestrand, C., Kleman, J., Heyman, J., Fabel, D., Fredin, O., Goodfellow, B. W.,
Harbor, J. M., Jansen, J. D., Olsen, L., Caffee, M. W., Fink, D., Lundqvist, J., Rosqvist, G.
C., Strömberg, B. Jansson, K. N. Deglaciation of Fennoscandia. Quaternary Science
Reviews, 147, 91-121. 2016.

1340   Tedstone, A.J. Nienow, P.W. Gourmelen, N. Dehecq, A. Goldberg, D. Hanna, E. Decadal slow-
down of a land-terminating sector of the Greenland Ice Sheet despite warming. Nature.
526: 692 – 95. 2015.

Tedstone, A.J. Nienow, P.W. Gourmelen, N. Sole, A.J. Greenland ice sheet annual motion
1345   insensitive to spatial variations in subglacial hydraulic structure. Geophysical Research
Letters. 41: 8910-17. 2014.

Tedstone, A.J. Nienow, P.W. Sole, A.J. Mair, D.W. Cowton, T.R. Bartholomew, I.D. et al.,
Greenland ice sheet motion insensitive to exceptional meltwater forcing. Proceedings of

1350   the National Academy of Sciences of the United States of America. 110(49). 19719–24.
        2013.

Utting, D.J., Ward, B.C. Little, E.C. Genesis of hummocks in glaciofluvial corridors near the
        Keewatin Ice Divide, Canada. Boreas. 38(3). 471–481. 2009.
1355

Van der Vegt, P., Janszen, A. Moscariello, A. Tunnel valleys: current knowledge and future
        perspectives. Geological Society, London, Special Publications. 368(1). 75–97. 2012.

van de Wal, R.S.W. Boot, W. Van den Broeke, M.R. Smeets, C.J.P.P. Reijmer, C.H. Donker, J.J.A.
1360   et al., Large and rapid melt-induced velocity changes in the ablation zone of the Greenland
        Ice Sheet. Science. 321. 111-13. 2008.

van de Wal, R.S.W. Smeets, C.J.P.P. Boot, W. Stoffelen, M. van Kampen, R. Doyle, S.H. et al.,
        Self-regulation of ice flow varies across the ablation area in south-west Greenland.
1365   Cryospehre. 9: 603-11. 2015.

Walder, J.S. Hydraulics of subglacial cavities. Journal of Glaciology. 32(112). 439-445. 1986.

Walder, J.S. Fowler, A. Channelized subglacial drainage over a deformable bed. Journal of
1370   Glaciology. 40(134). 1994.

Ward, B.C. Dredge, L.A. Kerr, D.E. Surficial geology, Lac de Gras, District of Mackenzie, Northwest
        Territories (NTS 76-D): Geological Survey of Canada, 1:125 000. 1997.

1375   Warren, W.P. Ashley, G.M. Origins of the ice-contact stratified ridges (eskers) of Ireland. Journal
        of Sedimentary Research. 64(3a). 433-49. 1994.

Weertman, J. General theory of water flow at the base of a glacier or ice sheet. Reviews of
        Geophysics and Space Physics. 10. 287-333. 1972.
1380

Werder, M.A. Hewitt, I.J Schoof, C.G. Flowers, G.E. Modeling channelized and distributed
        subglacial drainage in two dimensions. Journal of Geophysical Research: Earth Surface.
        118(4). .2140–58. 2013.

1385   Wheeler, J.O. Hoffman, P.F. Card, K.D. Davidson, A. Sanford, B.V. Okulitch, A.V. Roest, W.R.
        Geological Map of Canada. Geological Survey of Canada, map 1860A. 1996.

Zwally, H.J. Abdalati, W. Herring, T. Larson, K. Saba, J. Steffen, K. Surface melt induced
        acceleration of the Greenland Ice Sheet flow. Science. 297. 218-22. 2002.
1390

1395

9. Appendices
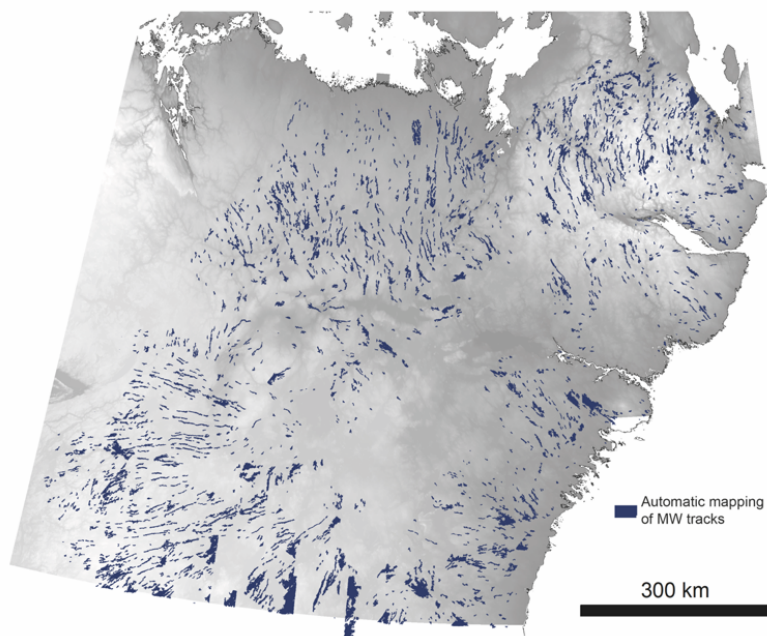
1400   **Figure A1**. Automatic mapping output (cleaned up) for test site using code associated with
Lewington et al., 2019.
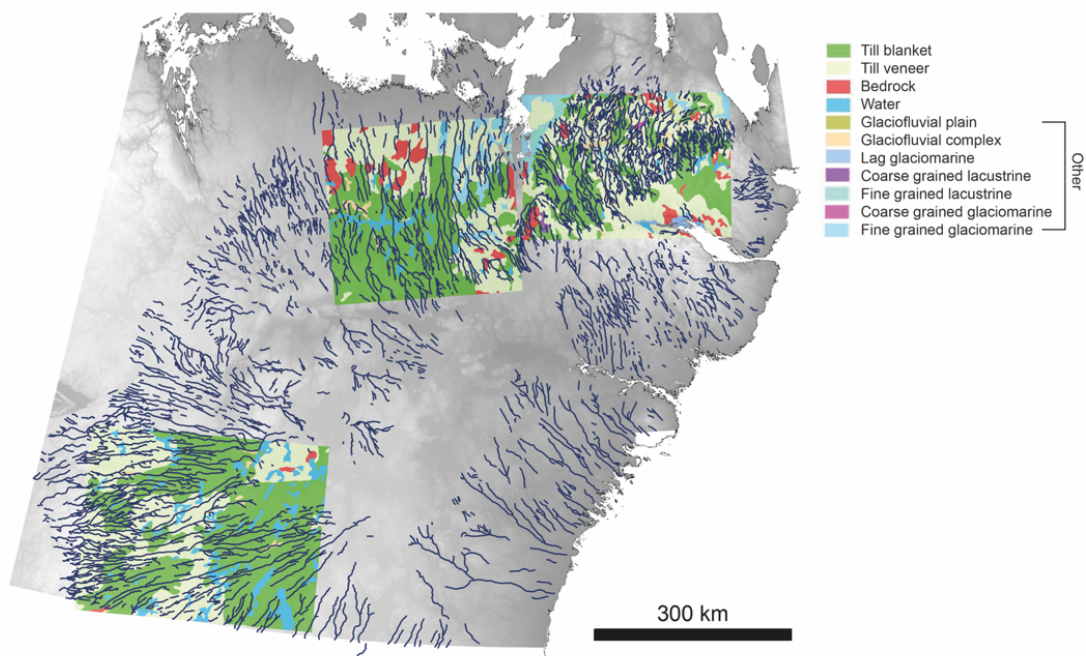
1405   **Figure A2.** Surface substrate across the three test sites (left – right) used for analysis in section 3.3
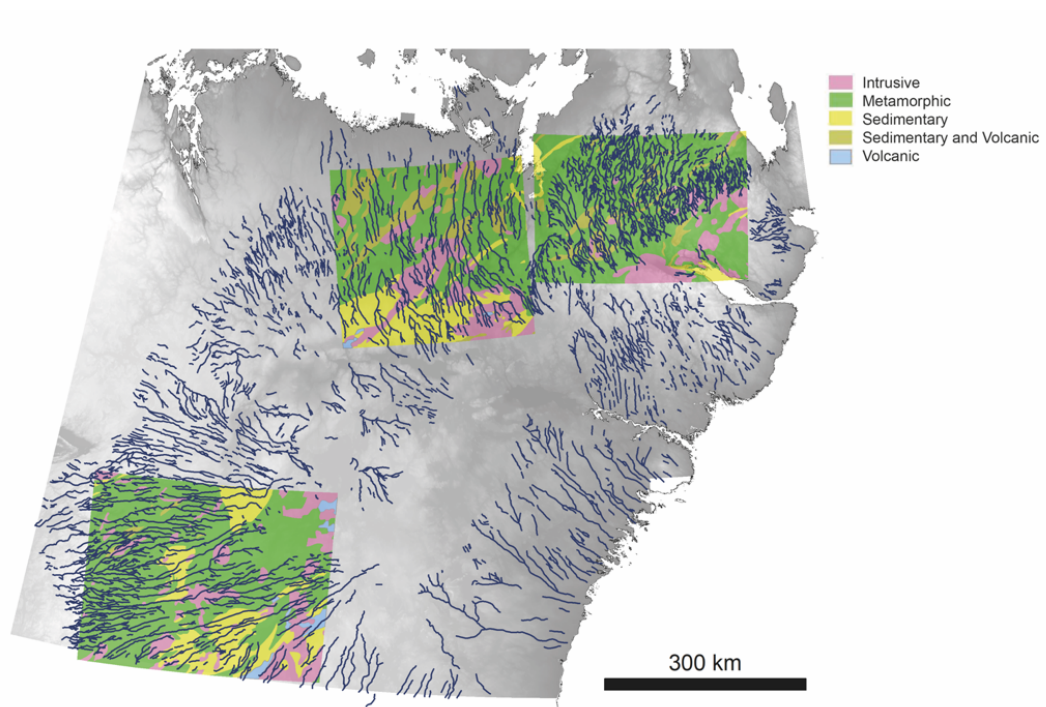
Figure A3. Bed geology across the three test sites (left to right) used for analysis in section 3.3